

# A Three-Parameter Model for Dark Matter Halos based on General Relativity and Quantum Field Theory

Jorge L. deLyra\*

Universidade de São Paulo  
Instituto de Física  
Rua do Matão, 1371,  
05508-090 São Paulo, SP, Brazil

July 11, 2024

## Abstract

We present a three-parameter model for the distributions of “dark matter” around local spherically symmetric and static distributions of normal matter, usually referred to as “dark matter halos”. The model is based on the assumption that the spontaneous symmetry breaking mechanism involving the Higgs field in the standard model of elementary particle physics leads to the existence of a constant distribution of vacuum energy throughout spacetime. This is to be interpreted as a constant distribution of *proper* energy, as measured by local observers in their proper reference frames. Due to the presence of this universal distribution of vacuum energy, the model requires the introduction of the cosmological term in the Einstein field equations, in order to regulate the behavior of the resulting geometry at cosmologically large distances.

By implementing the model on galactic scales, we are able to establish the gravitational consequences of such a homogeneous distribution of proper energy density at these scales. This results in equivalent halo masses and orbital velocity curves that, at least qualitatively, match the observations for galactic “dark matter” halos. Although the detailed realization of the model presented and calculated here cannot be construed as a precise representation of galactic structure, given that most of the actual structure of the galaxy, such as the galactic disk itself, is ignored, and replaced by a single spherically symmetric bulge, in this paper we do introduce the conceptual framework that may be used to construct a more complete galactic model in the future.

---

\*Email: delyra@lmail.if.usp.br ORCID: 0000-0002-8551-9711

**Keywords:**

General Relativity, Einstein Equations, Proper Density, Dark Matter, Velocity Curves, Quantum Field Theory, Higgs Field, Vacuum Expectation Value.

**DOI:** 10.5281/zenodo.12658035

# 1 Introduction

It is a well-established fact that the quantum field theory that underlies the standard model of elementary particles physics predicts the existence of an uncharged scalar field, the Higgs field, which for our purposes here may or may not be considered to be a fundamental one, and which has a non-zero vacuum expectation value. This is a consequence of the spontaneous symmetry breaking mechanism that is an essential part of the structure of that model, which is an universal model, and should therefore be associated with an universal distribution of energy density in the vacuum. In this paper we will assume the existence of such an energy distribution, and establish some of its consequences regarding the solutions of the Einstein field equations of general relativity. While the discussion of homogeneous distributions of vacuum energy is commonplace in cosmological arguments involving very large scales, here we will examine its possible consequences at *galactic* scales.

In flat spacetime the expectation value of the Higgs field is thought to be a constant throughout spacetime, that has the important role of generating the masses of all the massive particles appearing in the standard model. In this way this quantum scalar field shapes the underlying quantum-field-theoretical structure of the standard model. However, its vacuum expectation value in itself has no direct role when it comes to participating in interactions with other particles, associated with other quantum fields, specially in the case of the electromagnetic interactions, given that after the symmetry breaking is done the Higgs field carries no electric charge. The distribution of vacuum energy associated with this vacuum expectation value is therefore essentially invisible, transparent to light, and does not interact electromagnetically directly with charged matter. It must, however, undergo gravitational interactions, just like any other form of energy. This makes it a natural candidate for the constitution of the halos of so-called “dark matter” that are observed in nature, at galactic scales and above. We will keep this habitual name within quotes because, as one can plainly see, in the context of this model the actual physical object involved is neither dark nor made of matter, so that this commonplace reference becomes no more than a misnomer. A more descriptive name would be “transparent energy”.

We will assume the fundamental hypothesis that the expectation value of the Higgs field and the associated vacuum energy density are constant in curved spacetime as well, if measured in the tangent space at each point of the spacetime manifold. In other words, we will assume that all local observers measure the same amount of *proper* energy density of the vacuum, in their proper local reference frames. This must be so because the expectation value of the Higgs field determines all the masses and wavelengths (or correlation lengths in the Euclideanized version of the quantum field theory) around each given point of spacetime, and thus must be constant at all points, since the local physics of fields and particles is the same at all points. Therefore, the same must be true of the vacuum energy density that follows from it. In order to present the ideas in this paper in a more easily understandable way, it will be necessary to review some of the most basic facts about the symmetry breaking mechanism of the quantum field theory of the standard model, as well as some aspects of the structure and notation of general relativity.

This paper is organized as follows: in Section 2 we review just a few essential facts about the symmetry breaking mechanism of the quantum field theory of the standard model; in Section 3 we review succinctly the essentials of general relativity in regard to the particular type of static and spherically symmetric problem to be considered here; in Section 4 we present the conceptual definition of our model; in Section 5 we detail the development of our model for numerical purposes; in Section 6 we present and discuss the numerical results; and in Section 7 we present our conclusions and discuss the outlook.

## 2 Some Notes on Quantum Field Theory

Here we will discuss heuristically the origin of the proper energy density of the vacuum, as a consequence of spontaneous symmetry breaking in quantum field theory. More complete discussions, covering all the details, can be found in the advanced textbooks [1, 2]. For simplicity, in this section we will adopt the usual field-theoretical convention that  $\hbar = c = 1$  for the Planck constant  $\hbar$  and the speed of light  $c$ . Consider the Lagrangian density of a scalar field  $\Phi(x)$ , where the argument  $x$  stands for the four-vector  $x^\mu$ , with a quartic self-interaction term, such as we find in the scalar sector of the standard model, in flat four-dimensional spacetime,

$$\mathcal{L}[\Phi(x)] = \frac{1}{2} g^{\mu\nu} [\partial_\mu \Phi(x)] [\partial_\nu \Phi(x)] - \frac{m^2}{2} \Phi^2(x) - \frac{\lambda}{4} \Phi^4(x), \quad (1)$$

where the parameter  $m$  has the physical dimensions of inverse length and the positive self-coupling parameter  $\lambda$  is dimensionless. Instead of the single scalar component shown here, this scalar field could carry an internal symmetry group index, such as for a representation of the  $U(1)$  or  $SU(2)$  symmetry groups, having therefore several scalar components, without any qualitative change in the argument that follows. This Lagrangian density  $\mathcal{L}[\Phi(x)]$  has the same physical dimensions as that of the corresponding Hamiltonian density  $\mathcal{H}[\Phi(x)]$ , which is obtained from it by a Legendre transformation, resulting in an expression in which all terms are now positive, given that  $g^{ij}$  is the negative of the positive-definite three-dimensional spatial metric,

$$\mathcal{H}[\Phi(x)] = \frac{1}{2} g^{00} [\partial_0 \Phi(x)]^2 - g^{ij} [\partial_i \Phi(x)] [\partial_j \Phi(x)] + \frac{m^2}{2} \Phi^2(x) + \frac{\lambda}{4} \Phi^4(x), \quad (2)$$

namely the physical dimensions of energy density, so that the three-dimensional integrals giving the Lagrangian function  $L[\Phi(t)]$  and the Hamiltonian energy function  $H[\Phi(t)]$ ,

$$L[\Phi(t)] = \int_V d^3x \mathcal{L}[\Phi(x)], \quad (3)$$

$$H[\Phi(t)] = \int_V d^3x \mathcal{H}[\Phi(x)], \quad (4)$$

over a volume  $V$ , have the physical dimensions of energy. Spontaneous symmetry breaking of the reflection symmetry  $\Phi(x) \rightarrow -\Phi(x)$  of the scalar field (or of the corresponding  $U(1)$  or  $SU(2)$  symmetries) comes about when we make  $m^2$  negative. If we assume that the resulting vacuum expectation value  $\langle \Phi(x) \rangle = \vartheta$  is a non-zero real constant, independent of  $x^\mu$ , which is given approximately by  $\vartheta = \sqrt{-m^2/\lambda}$ , and shift the field as  $\Phi'(x) = \Phi(x) - \vartheta$ , so that we have  $\Phi(x) = \Phi'(x) + \vartheta$  with  $\langle \Phi'(x) \rangle = 0$ , then we get for the Lagrangian density

$$\begin{aligned} \mathcal{L}[\Phi'(x)] &= \frac{1}{2} g^{\mu\nu} [\partial_\mu \Phi'(x)] [\partial_\nu \Phi'(x)] \\ &\quad - \frac{m^2}{2} [\Phi'^2(x) + 2\vartheta \Phi'(x) + \vartheta^2] \\ &\quad - \frac{\lambda}{4} [\Phi'^4(x) + 4\vartheta \Phi'^3(x) + 6\vartheta^2 \Phi'^2(x) + 4\vartheta^3 \Phi'(x) + \vartheta^4]. \end{aligned} \quad (5)$$

Note that the concept of vacuum state being employed here is that of the *particle vacuum*, as defined in quantum field theory. These transformations result in the presence of a field-independent term  $\Delta\mathcal{L}$  of  $\mathcal{L}[\Phi'(x)]$ , and also in a corresponding field-independent term  $\Delta\mathcal{H}$  of  $\mathcal{H}[\Phi'(x)]$ , such that we have  $\Delta\mathcal{H} = -\Delta\mathcal{L}$ , given by

$$\Delta\mathcal{H} = \frac{m^2\vartheta^2}{2} + \frac{\lambda\vartheta^4}{4}, \quad (6)$$

which is a term devoid of quantum fluctuations, that therefore constitutes a classical energy density distributed throughout the vacuum. Note that in the broken-symmetric scenario the squared mass term will become negative, but that the quartic term is still positive. Independently of the details of the expressions above, the main point is that a classical energy density appears over the whole of spacetime, due to the spontaneous symmetry breaking mechanism. It is noteworthy that further contributions to this energy density may also arise from the quantum fluctuations of the field  $\Phi(x)$ .

At this point it is important to note that one can add any field-independent constant term to the Lagrangian density  $\mathcal{L}[\Phi(x)]$  without changing either the classical field theory corresponding to it or the quantum field theory generated by it, according to the usual representation of the latter in terms of functional integrals. In the case of the classical theory, any such constant term will be eliminated by the derivatives with respect to the field that appear in the Euler-Lagrange equation,

$$\frac{\partial\mathcal{L}[\Phi]}{\partial\Phi} - \partial_\mu \frac{\partial\mathcal{L}[\Phi]}{\partial[\partial_\mu\Phi]} = 0, \quad (7)$$

which leads to the classical equation of motion. In the case of the quantum theory, this term is equivalent to a normalization constant that will always cancel out in the ratios of functional integrals giving the expectation values of arbitrary observables  $\mathcal{O}[\Phi]$ ,

$$\begin{aligned} \langle\mathcal{O}\rangle &= \frac{\int [d\Phi] \mathcal{O}[\Phi] e^{iS[\Phi]}}{\int [d\Phi] e^{iS[\Phi]}} \\ &= \frac{\int [d\Phi] \mathcal{O}[\Phi] e^{i\int d^4x \mathcal{L}[\Phi]}}{\int [d\Phi] e^{i\int d^4x \mathcal{L}[\Phi]}} \\ &= \frac{\cancel{e^{i\int d^4x \Delta\mathcal{L}}} \int [d\Phi] \mathcal{O}[\Phi] e^{i\int d^4x \mathcal{L}'[\Phi]}}{\cancel{e^{i\int d^4x \Delta\mathcal{L}}} \int [d\Phi] e^{i\int d^4x \mathcal{L}'[\Phi]}}, \end{aligned} \quad (8)$$

where

$$S[\Phi] = \int d^4x \mathcal{L}[\Phi] \quad (9)$$

is the action functional, and the functional integrals are sums over all possible field configurations, that is, over all possible functions  $\Phi(x)$ . Here the shifted Lagrangian density  $\mathcal{L}'[\Phi(x)] = \mathcal{L}[\Phi(x)] - \Delta\mathcal{L}$  does not contain any field-independent terms, and the factors containing  $\Delta\mathcal{L}$  can be put in evidence in the functional integrals, since they do not depend on  $\Phi(x)$ , and hence cancel out after that. Therefore, neither the classical theory nor the quantum theory in flat spacetime determine this constant term. Only gravitation would depend on its presence, and here we will simply assume that it has some positive and non-zero value, so that the symmetry breaking mechanism results in a positive universal energy density of the vacuum. The determination of this value will be left to future comparisons of results obtained from this model with astronomical observations.

### 3 Some Notes on General Relativity

Here we will review some elements of the formalism of general relativity and of the geometry of curved spacetime. Expositions of the whole theory, in all its extension and in great detail, can be found in many well-known advanced textbooks [3–5]. Writing the Einstein field equations with the inclusion of the so-called cosmological term, involving the cosmological constant  $\Lambda$ , we have

$$R_\mu^\nu - \frac{1}{2} R g_\mu^\nu + \Lambda g_\mu^\nu = -\kappa T_\mu^\nu, \quad (10)$$

where  $\kappa = 8\pi G/c^4$ ,  $G$  is the universal gravitational constant and  $c$  is the speed of light. In the context of our model we will interpret  $T_\mu^\nu$  as the stress-energy tensor of the vacuum. As one can see above, in this paper we will use the time-like signature  $(+, -, -, -)$ , following [3]. Rescaling  $\Lambda$  by the constant  $\kappa$ , that is, making  $\rho_\Lambda = \Lambda/\kappa$ , and making therefore  $\Lambda = \kappa\rho_\Lambda$ , where  $\rho_\Lambda$  turns out to have the physical dimensions of energy density, we can pass the cosmological term to the source side of the equation, thus obtaining

$$\begin{aligned} R_\mu^\nu - \frac{1}{2} R g_\mu^\nu &= -\kappa (T_\mu^\nu + \rho_\Lambda g_\mu^\nu) \\ &= -\kappa \mathcal{T}_\mu^\nu, \end{aligned} \quad (11)$$

where we have defined the total stress-energy tensor as the sum  $\mathcal{T}_\mu^\nu = T_\mu^\nu + \rho_\Lambda g_\mu^\nu$ . Note that, although  $\rho_\Lambda$  has the physical dimensions of energy density, it is *not* really an energy density, since it does not transform in the correct way under coordinate transformations. It is still a scalar, just like  $\Lambda$ , and therefore transforms as such, rather than as the  $T_0^0$  component of a rank-2 stress-energy tensor, as does the energy density. In Schwarzschild coordinates  $(ct, r, \theta, \phi)$ , in which the invariant interval is given by

$$ds^2 = e^{2\nu(r)} c^2 dt^2 - e^{2\lambda(r)} dr^2 - r^2 [d\theta^2 + \sin^2(\theta) d\phi^2], \quad (12)$$

where  $\exp[2\nu(r)]$  and  $\exp[2\lambda(r)]$  are two positive functions of only  $r$ , for static and spherically symmetric solutions, the vacuum stress-energy tensor  $T_\mu^\nu$  appearing in this expression is diagonal, with the diagonal components given by

$$\text{diag} [T_\mu^\nu] = [\rho(r), -P(r), -P(r), -P(r)], \quad (13)$$

where  $\rho(r)$  is the energy density of the vacuum, and  $P(r)$  is its pressure, which is isotropic, as is required for any isotropic medium, such as a fluid, for example, while the cosmological term is also diagonal, given simply by

$$\text{diag} [\rho_\Lambda g_\mu^\nu] = [\rho_\Lambda, \rho_\Lambda, \rho_\Lambda, \rho_\Lambda], \quad (14)$$

so that the total stress-energy tensor  $\mathcal{T}_\mu^\nu$  shown on the right-hand side of Equation (11) is given by the matrix

$$\mathcal{T}_\mu^\nu = \begin{bmatrix} \rho(r) + \rho_\Lambda & 0 & 0 & 0 \\ 0 & -P(r) + \rho_\Lambda & 0 & 0 \\ 0 & 0 & -P(r) + \rho_\Lambda & 0 \\ 0 & 0 & 0 & -P(r) + \rho_\Lambda \end{bmatrix}. \quad (15)$$

Therefore, in this situation the result of the addition of the cosmological term, to the theory originally without that term, can be obtained by the simple transformations

$$\rho(r) \longrightarrow \rho(r) + \rho_\Lambda, \quad (16)$$

$$P(r) \longrightarrow P(r) - \rho_\Lambda, \quad (17)$$

where  $\rho_\Lambda$  is presumed to be an universal physical constant. In [6] we showed that the field equations in Equation (11) without the cosmological term can be reduced, in the static and spherically symmetric case, in Schwarzschild coordinates, to the set of three first-order differential equations

$$[1 - 2r\lambda'(r)] e^{-2\lambda(r)} = 1 - \kappa r^2 \rho(r), \quad (18)$$

$$[1 + 2r\nu'(r)] e^{-2\lambda(r)} = 1 + \kappa r^2 P(r), \quad (19)$$

$$[P(r) + \rho(r)] \nu'(r) = -P'(r), \quad (20)$$

where the primes indicate differentiation with respect to  $r$  and where Equation (20) above is a consistency condition derived from the Bianchi identity of the Ricci curvature tensor. Note that the left-hand side of Equation (18) above can be written as a total derivative. If we now use the transformations given in Equations (16) and (17), we get

$$[1 - 2r\lambda'(r)] e^{-2\lambda(r)} = 1 - \kappa r^2 [\rho(r) + \rho_\Lambda], \quad (21)$$

$$[1 + 2r\nu'(r)] e^{-2\lambda(r)} = 1 + \kappa r^2 [P(r) - \rho_\Lambda], \quad (22)$$

$$[P(r) + \rho(r)] \nu'(r) = -P'(r). \quad (23)$$

Note that Equation (23) above does not change in this transformation because  $\rho_\Lambda$  is a constant, so that  $\rho'_\Lambda = 0$ , and because the terms involving  $\rho_\Lambda$  cancel off in its left-hand side. If we now transform to a dimensionless radial variable  $\xi$ , as well as to dimensionless versions of the constant  $\rho_\Lambda$  and of the functions  $\rho(r)$  and  $P(r)$ , given by

$$\xi = r/r_0, \quad (24)$$

$$\bar{\rho}_\Lambda = \kappa r_0^2 \rho_\Lambda, \quad (25)$$

$$\bar{\rho}(\xi) = \kappa r_0^2 \rho(\xi), \quad (26)$$

$$\bar{P}(\xi) = \kappa r_0^2 P(\xi), \quad (27)$$

where  $r_0$  is an arbitrary reference value, a fixed radial position, that for the time being remains unspecified, then we can write these three differential equations as

$$[\xi e^{-2\lambda(\xi)}]' = 1 - \xi^2 [\bar{\rho}(\xi) + \bar{\rho}_\Lambda], \quad (28)$$

$$[1 + 2\xi\nu'(\xi)] e^{-2\lambda(\xi)} = 1 + \xi^2 [\bar{P}(\xi) - \bar{\rho}_\Lambda], \quad (29)$$

$$\nu'(\xi) = -\frac{\bar{P}'(\xi)}{\bar{P}(\xi) + \bar{\rho}(\xi)}, \quad (30)$$

where the primes now indicate differentiation with respect to  $\xi$ . Using a transformation of variables from the metric function  $\lambda(\xi)$  to a new function  $\gamma(\xi)$  given by the relation

$$e^{2\lambda(\xi)} = \frac{\xi}{\xi - \gamma(\xi)}, \quad (31)$$

we get for our three field equations, now in terms of the function  $\gamma(\xi)$ ,

$$\gamma'(\xi) = \xi^2 [\bar{\rho}(\xi) + \bar{\rho}_\Lambda], \quad (32)$$

$$\nu'(\xi) = \frac{\gamma(\xi) + \xi^3 [\bar{P}(\xi) - \bar{\rho}_\Lambda]}{2\xi [\xi - \gamma(\xi)]}, \quad (33)$$

$$\nu'(\xi) = -\frac{\bar{P}'(\xi)}{\bar{P}(\xi) + \bar{\rho}(\xi)}. \quad (34)$$

From the two equations above for  $\nu'(\xi)$  we get an equation for  $\bar{P}'(\xi)$ , by simply eliminating  $\nu'(\xi)$ , thus obtaining

$$\bar{P}'(\xi) = - \frac{\gamma(\xi) + \xi^3 [\bar{P}(\xi) - \bar{\rho}_\Lambda]}{2\xi [\xi - \gamma(\xi)]} [\bar{P}(\xi) + \bar{\rho}(\xi)]. \quad (35)$$

We have therefore the set of three first-order differential equations

$$\gamma'(\xi) = \xi^2 [\bar{\rho}(\xi) + \bar{\rho}_\Lambda], \quad (36)$$

$$\bar{P}'(\xi) = - \frac{\gamma(\xi) + \xi^3 [\bar{P}(\xi) - \bar{\rho}_\Lambda]}{2\xi [\xi - \gamma(\xi)]} [\bar{P}(\xi) + \bar{\rho}(\xi)], \quad (37)$$

$$\nu'(\xi) = \frac{\gamma(\xi) + \xi^3 [\bar{P}(\xi) - \bar{\rho}_\Lambda]}{2\xi [\xi - \gamma(\xi)]}. \quad (38)$$

This is the basic set of field equations which is relevant to the current problem, still with no particular choices regarding the values of the constant  $\bar{\rho}_\Lambda$  and of the function  $\bar{\rho}(\xi)$ , as well as of the boundary and asymptotic conditions for the functions  $\gamma(\xi)$ ,  $\bar{P}(\xi)$  and  $\nu(\xi)$ . Discussions of these choices will be given in the next two sections. Note that, since these are first-order differential equations, there is only one relevant boundary condition to be imposed on each one of the three quantities involved, namely the conditions of the continuity of  $\gamma(\xi)$ ,  $\bar{P}(\xi)$  and  $\nu(\xi)$  across interfaces.

As a last preparatory development, we must consider here the geodesic equation. This will be used for the calculation of the orbital velocity of a test particle in a circular orbit around the origin, as a function of the radial coordinate  $r$ . In its most general form the equation can be written as

$$\frac{\partial^2}{\partial \tau^2} x^\mu = \Gamma^\mu_{\nu\sigma} \left( \frac{\partial x^\nu}{\partial \tau} \right) \left( \frac{\partial x^\sigma}{\partial \tau} \right), \quad (39)$$

where  $x^\mu$  are the coordinates of the test particle and  $\tau$  is its proper time. Note that any other monotonic parameter along the geodesic curves can be used in place of the proper time  $\tau$  in this equation. If we write  $x^\mu$  in the Schwarzschild coordinate system we get

$$\begin{aligned} x^\mu &= (x^0, x^1, x^2, x^3) \\ &= (ct, r, \theta, \phi), \end{aligned} \quad (40)$$

and then the geodesic equation, using  $t$  as the parameter, can be written as

$$\frac{\partial^2}{\partial t^2} x^\mu = \Gamma^\mu_{\nu\sigma} \left( \frac{\partial x^\nu}{\partial t} \right) \left( \frac{\partial x^\sigma}{\partial t} \right). \quad (41)$$

We will assume that the orbits are in the equatorial plane, so that  $\theta = \pi/2$  is a constant, with  $\sin(\theta) = 1$ , and also that they are circular, so that  $r$  is also a constant. We therefore have for the coordinates of the test particle, with all the dependencies on  $t$  made explicit,

$$x^\mu = (ct, r, \pi/2, \phi(t)), \quad (42)$$

so that only  $x^0$  and  $x^3$  depend on  $t$ . Hence only the values 0 and 3 of  $\nu$  and  $\sigma$  appear in Equation (41), in which we have that

$$\frac{\partial x^0}{\partial t} = c, \quad (43)$$

$$\frac{\partial x^3}{\partial t} = \dot{\phi}(t), \quad (44)$$



where the dot over the symbol indicates differentiation with respect to the time, and hence the geodesic equation reduces to

$$\frac{\partial^2}{\partial t^2} x^\mu = \Gamma_{00}^\mu c^2 + 2\Gamma_{03}^\mu c \dot{\phi}(t) + \Gamma_{33}^\mu \dot{\phi}^2(t). \quad (45)$$

For the values  $\mu = 0$  and  $\mu = 2$  this reduces to identities, as can be verified with the use of the values of the Christoffel connection components  $\Gamma_{\nu\sigma}^\mu$  given in Appendix A. For the value  $\mu = 3$  it reduces to  $\ddot{\phi}(t) = 0$ , and hence to the statement that the angular velocity  $\dot{\phi}(t)$  is a constant, which is just an expression of the conservation of angular momentum. For the value  $\mu = 1$ , defining the orbital velocity as  $v_\phi = r\dot{\phi}$ , as required by the invariant interval in Schwarzschild coordinates, since for  $t$ ,  $r$  and  $\theta = \pi/2$  constant we can obtain from Equation (12) that the spatial arc length along  $\phi$  is given by  $d\ell = r d\phi$ , we get

$$\begin{aligned} v_\phi^2 &= \frac{c^2}{2} r \frac{\partial}{\partial r} e^{2\nu(r)} \\ &= \frac{c^2}{2} \xi \frac{\partial}{\partial \xi} e^{2\nu(\xi)} \\ &= c^2 \xi \nu'(\xi) e^{2\nu(\xi)}, \end{aligned} \quad (46)$$

where the prime indicates differentiation with respect to  $\xi$ . Therefore, from the geodesic equation we have for the orbital velocity  $v_\phi(\xi)$ , for a circular orbit at the radial position  $\xi$ ,

$$v_\phi(\xi) = c \sqrt{\xi \nu'(\xi)} e^{\nu(\xi)}. \quad (47)$$

This is the expression that will give the velocity curves determined by the solutions of our model, once  $\nu(\xi)$  is obtained. As a simple example, we may use this for the case of the exterior Schwarzschild solution with asymptotic gravitational mass  $M$ , in which we have that  $\exp[2\nu(\xi)] = 1 - \xi_M/\xi$ , where  $\xi_M = r_M/r_0$  is the rescaled Schwarzschild radius  $r_M = 2GM/c^2$  associated with the mass  $M$ , leading at once to the well-known simple result

$$v_\phi(\xi) = c \sqrt{\frac{\xi_M}{2\xi}}, \quad (48)$$

which in terms of dimensionfull variables and functions can be written as

$$v_\phi(r) = \sqrt{\frac{MG}{r}}, \quad (49)$$

and which is, in fact, exactly the same as the classical Newtonian result. This represents a definite but rather slow fall to zero as  $r \rightarrow \infty$ .

Note that from Equations (36) through (38) it follows that, while  $\gamma(\xi)$  (and therefore  $\lambda(\xi)$ ) can be determined without any reference to either  $\bar{P}(\xi)$  or  $\nu(\xi)$ , the metric function  $\nu(\xi)$  depends on both  $\gamma(\xi)$  and  $\bar{P}(\xi)$ . Note also that  $\bar{P}(\xi)$  depends on  $\gamma(\xi)$  but can be obtained without any reference to  $\nu(\xi)$ . Therefore, the result of the operation indicated above will depend on the initial conditions used for the integration of the equation for  $\bar{P}(\xi)$ . It will also depend on the initial conditions used for the integration of the equation for  $\nu(\xi)$ , but those are easily determined when integrating backward from some exterior radial position, given the interface boundary conditions that connect the solution obtained from these equations to the exterior Schwarzschild solution, which we will assume to be valid beyond that exterior radial position, as will be discussed in detail in Section 5. Note that the exterior Schwarzschild solution is itself a vacuum solution of the field equations, where the concept of the vacuum in this case is that used in general relativity, meaning an *absolute vacuum* within which there is the absence of any form of non-gravitational energy.

## 4 Conceptual Definition of the Model

The basic idea that we will use here, coming from quantum field theory, is that the spontaneous symmetry breaking mechanism involving the vacuum expectation value  $\langle\Phi\rangle$  of the Higgs field gives origin to an homogeneous distribution of vacuum energy  $\rho_H$  throughout spacetime. Since this expectation value defines the masses of all massive particles, as well as all the associated wavelengths, it therefore defines all physical notions of length, and hence determines the metrical geometry of spacetime. Since the physics of particles and fields is the same at all points of spacetime, this distribution of energy should be considered as being intrinsically and conceptually homogeneous across all points of spacetime, even if this spacetime is curved. This implies that  $\rho_H$  should be an homogeneous distribution of *proper* energy density, as seen and measured within the flat tangent space at each point of the spacetime manifold.

At this point it is necessary to establish a clear distinction between the two concepts of vacuum that are at play here. On the one hand, we have the *particle vacuum* of quantum field theory, that is defined as the state within a given region in which we have the complete absence of any particles or, in other words, the complete absence of any excitations of the quantum fields, which are what we usually describe as particles. In general-relativistic terms, this condition is equivalent to the absence of normal matter. On the other hand, we have the *absolute vacuum* of general relativity, which is defined as the absence of any non-gravitational energy in a region of spacetime. This is the vacuum in which the exterior Schwarzschild solution exists. The point of this paper could be expressed as the consideration of the possibility that we may have a particle vacuum that is *not* an absolute vacuum, due to the presence of the non-zero vacuum expectation value of the Higgs field.

Note that since the quantum field theory of the standard model is an universal theory, supposed to describe the whole of the material universe, if it does really produce a non-zero vacuum energy density throughout spacetime, then in principle the absolute vacuum of general relativity simply does not exist. However, as we will see, we may adjust the parameters of the Einstein theory so that there are regions where an absolute vacuum does exist, devoid of any matter and of any net amount of vacuum energy density. From now on, we will reserve the simple term *vacuum* to mean the particle vacuum of quantum field theory, and will use explicitly the term *absolute vacuum* when we mean the vacuum as defined in general relativity, meaning the absence of any normal matter and of any vacuum energy density associated with either the Higgs field or the cosmological constant.

We are going to assume that both localized distributions of normal matter and this global distribution of vacuum energy contribute to the curvature of spacetime, that is, to the gravitational field, as would be indicated by Equation (10) if we were to use for the  $T_\mu^\nu$  tensor appearing there the sum of the stress-energy tensors of the normal matter and of the vacuum. However, in the absence of any normal matter, this global distribution of vacuum energy can cause only global curvature of spacetime, of a cosmological nature, and not localized curvature around any particular point, as a direct consequence of the fact that it is global and homogeneous. By simple invariance arguments, given the rotational and translational symmetries of empty spacetime in the absence of any normal matter, under these circumstances the generation of local gravitational fields by such an homogeneous universal distribution of vacuum energy, such as the localized gravitational fields that exist around stars and galaxies, is clearly not possible.

On the other hand, once a localized distribution of normal matter has broken the global translational and rotational symmetries, then this global homogeneous vacuum energy density can have detectable gravitational effects in the vicinity of the normal matter distribu-

tion. Note, however, that this is *not* because the vacuum energy becomes more concentrated at any particular position. Its proper density is homogeneous *by definition*, and continues to be a constant in each local system of proper coordinates, at all points. However, because due to the curvature of space there is more proper volume in the vicinity around and immediately outside the local distribution of normal matter, than in the corresponding flat space, the apparent density in Schwarzschild coordinates will not be homogeneous, and will in fact increase in the vicinity of the normal matter. It is this geometrical phenomenon that leads to the observable gravitational effects of the distribution of vacuum energy.

It is important to observe that the absence of local gravitational effects in the case of an universal homogeneous distribution of vacuum energy, although made clear by the symmetry arguments, is not easily accessible through a local analysis around any given point of spacetime. This is because the symmetry argument only holds if the whole of spacetime is considered at once, and an integration outward from any given point will not achieve that at any stage of the limiting process to radial infinity. If we analyze the problem in this way, we just get more and more vacuum energy within the integration domain as we take its radius to radial infinity, and the integration diverges in that limit. Therefore, in order to treat the problem around some particular point where some amount of normal matter is concentrated, a carefully tailored mathematical procedure will be needed. For one thing, in order to eliminate the global curvature effects, that have only a cosmological meaning, which is not within the scope of this paper, as well as to allow the use of such a local analysis, we will have to introduce into the theory a cosmological term, as described in Section 3, in which the cosmological constant  $\Lambda$  has an appropriate value and sign.

#### 4.1 The Spherically Symmetric Case

From this point onward, in order to be able to guide the discussion, as much as possible, by means of the analysis of a concrete case, we will restrict the development of the model to the case in which we have spherical symmetry around a given point. As was already mentioned in Section 3, it is very important to emphasize that  $\Lambda$  is a scalar, and not an energy density, since that is given by the  $T_0^0$  component of a second-rank stress-energy tensor. While it is true that the constant  $\Lambda$  can be rescaled by the constant  $\kappa$  in order to result in the equivalent constant  $\rho_\Lambda$  that has the physical dimensions of energy density, in either form this quantity is still a scalar and hence does *not* transform in the correct way under changes of reference frame. It is also very important to emphasize that, as was already mentioned a couple of times before, in Sections 1 and 4, since the vacuum expectation value of the Higgs field defines all the physical masses and lengths, and therefore determines all possible length measurements and hence the metric geometry of spacetime, we have to assume that this distribution of vacuum energy has a constant value when expressed as a quantity of energy per unit of *proper* volume.

Therefore, when there is a localized distribution of normal matter, this distribution of vacuum energy will *not* be constant as a function of the radial coordinate  $\xi$  of a spherical system of coordinates around the matter, such as the Schwarzschild system of coordinates. If  $\rho(\xi)$  is this vacuum energy density for a spherically symmetric and static case, written in terms of the radially rescaled Schwarzschild coordinates  $(ct, \xi, \theta, \phi)$  around the center of the distribution of normal matter, and if  $\rho_H$  is the homogeneous proper energy density of the vacuum, then we have for this energy density that

$$\rho(\xi) = \rho_H e^{\lambda(\xi)}, \quad (50)$$

as was already discussed in some detail in a previous paper [7]. The argument leading

to this is as follows. Given an element of three-dimensional spatial *coordinate* volume  $\delta V_C = dr \times r d\theta \times r \sin(\theta) d\phi$ , if we make  $\rho(r) = \rho_0$  then  $\rho_0$  is the constant quantity of energy  $\delta E_C = \rho_0 \delta V_C$  per unit of *coordinate* spatial volume, so that

$$\delta E_C = \rho_0 r^2 \sin(\theta) dr d\theta d\phi. \quad (51)$$

However, as one can see in Equation (12), the element of *proper* spatial volume contained within this element of coordinate spatial volume is given by a different expression, which can be written as  $\delta V_P = \exp[\lambda(r)] dr \times r d\theta \times r \sin(\theta) d\phi$ , so that if  $\rho_H$  is a constant *proper* energy density, then it gives a constant amount of energy  $\delta E_P = \rho_H \delta V_P$  per unit of *proper* spatial volume, which is expressed as

$$\delta E_P = \rho_H r^2 e^{\lambda(r)} \sin(\theta) dr d\theta d\phi. \quad (52)$$

If we want to express this physical situation, namely that of a homogeneous distribution of proper density of energy, in terms of an energy density  $\rho(r)$  in Schwarzschild coordinates, then we must impose that  $\rho(r)$  results in  $\delta E_P = \rho(r) \delta V_C$  when taken in an element of coordinate volume  $\delta V_C$ , so that we have

$$\rho(r) r^2 \sin(\theta) dr d\theta d\phi = \rho_H r^2 e^{\lambda(r)} \sin(\theta) dr d\theta d\phi, \quad (53)$$

from which it follows at once that, in order to have a constant proper energy density  $\rho_H$ , we must have the form of  $\rho(r)$  given in Equation (50), in terms of the radial metric function  $\lambda(r)$ , and the same for  $\rho(\xi)$  and  $\lambda(\xi)$ . Therefore the expression in Equation (50) is the form of the energy density  $\rho(\xi)$ , expressed in the Schwarzschild system of coordinates, that corresponds to a constant proper energy density  $\rho_H$  of the vacuum, in a spherically symmetric setting. We will assume that  $\rho_H$ , just like  $\rho_\Lambda$ , is an universal physical constant.

Since, in order to facilitate the construction of a practical instance of our model, we will concentrate on the simple case of a spherically symmetric and static distribution of normal matter, we will therefore assume that we have a distribution of normal matter that is spherically symmetric and static, with total mass  $M_1$ . We will assume that this distribution exists within a sphere centered at the origin with its surface going through a certain interior radial position  $\xi_1 = r_1/r_0$ , that is such that  $\xi_1 > \xi_{M_1}$ , where  $\xi_{M_1} = r_{M_1}/r_0$  is the rescaled Schwarzschild radius  $r_{M_1} = 2GM_1/c^2$  of the total mass  $M_1$  of the normal matter. This radial position  $\xi_1$  could be the actual radius of the localized distribution of normal matter, or it could be somewhat larger than that.

The only condition that we impose on  $\xi_1$  is that all the normal matter be contained within the spherical surface centered at the origin and passing by that radial position. Therefore, the value of  $\xi_1$  is not one that can be obtained from this particular realization of the model. Outside this sphere at  $\xi_1$  we have just the universal distribution of vacuum energy with constant proper density, and no normal matter. This is the region within which we will endeavor to solve the field equations, and since we do not specify the details about the actual distribution of the normal matter, in principle the solution will be valid within the interval  $(\xi_{M_1}, \xi_2]$ , thus excluding only, at its left end, the position  $\xi_{M_1}$  of a possible event horizon formed by the mass  $M_1$ .

Looking back at Equation (36), we find on its right-hand side the motivation to define something that works effectively like a total energy density  $\rho_{\mathcal{T}}(\xi)$  of the vacuum, as the sum of the cosmological term  $\rho_\Lambda$  with dimensions of energy density and of the energy density  $\rho(\xi)$  given in terms of  $\rho_H$  and originating from the expectation value of the Higgs field,

$$\begin{aligned} \rho_{\mathcal{T}}(\xi) &= \rho(\xi) + \rho_\Lambda \\ &= \rho_H e^{\lambda(\xi)} + \rho_\Lambda. \end{aligned} \quad (54)$$

This is functionally identical to the  $\mathcal{T}_0^0$  component of the total stress-energy tensor  $\mathcal{T}_\mu^\nu$  that appears in Equation (11). Although this quantity has a mixed tensorial nature, mixing a scalar with the  $T_0^0$  component of a second-rank tensor, it does have the role usually played by the energy density in the field equations written in the Schwarzschild system of coordinates, and thus we will name it the *effective total energy density* of the vacuum. Similarly, we have an *effective total pressure*  $P_{\mathcal{T}}(\xi)$  given by

$$P_{\mathcal{T}}(\xi) = P(\xi) - \rho_\Lambda, \quad (55)$$

but in this case there is no simple analytical form for  $P(\xi)$  in terms of the metric functions, and its form will only be obtained as part of the complete solution of the problem.

Let us now discuss the asymptotic behavior of the solutions at radial infinity. This is where we make our first important choice, that of the value of the constant  $\rho_\Lambda$ . We are going to assume that  $\rho_\Lambda$  is negative, with  $\rho_\Lambda = -\rho_H$ , so that these two quantities cancel one another in the flat space at radial infinity, where we expect that  $\lambda(\xi) \rightarrow 0$  and hence that  $\exp[\lambda(\xi)] \rightarrow 1$ , thus resulting in  $\rho_{\mathcal{T}}(\xi) = 0$  there. This is just the hypothesis that there still is a classical Newtonian limit asymptotically valid at radial infinity. Note that this means that the combined gravitational effects of the universal distribution of proper energy density  $\rho_H$  and of the cosmological constant  $\rho_\Lambda$  are given by the excess energy density, obtained when we subtract the constant  $\rho_H = -\rho_\Lambda$  from the energy density  $\rho(\xi)$ , as described by the effective total energy density  $\rho_{\mathcal{T}}(\xi)$  defined in Equation (54), which is now given by

$$\begin{aligned} \rho_{\mathcal{T}}(\xi) &= \rho(\xi) - \rho_H \\ &= \rho_H \left[ e^{\lambda(\xi)} - 1 \right]. \end{aligned} \quad (56)$$

Note that this is a positive quantity so long as  $\lambda(\xi) > 0$ , which is the case here since we have no event horizons in this type of very low-density solution. This quantity goes to zero when  $\xi \rightarrow \infty$ , where we expect that  $\lambda(\xi) \rightarrow 0$  and  $\exp[\lambda(\xi)] \rightarrow 1$ , and hence expect spacetime to be asymptotically flat. Note the similarity between  $\rho_\Lambda$  and a counter-term in renormalized quantum field theory. We might also refer to  $\rho_{\mathcal{T}}(\xi)$  as the *subtracted* energy density.

Since there is no normal matter involved in the region  $\xi \geq \xi_{M_1}$  within which we will solve the field equations, the usual statistical interpretation of the pressure  $P(\xi)$  appearing in Equation (13), in terms of the thermal agitation of molecules, atoms or ions, does not apply, so that in principle this function can be either positive or negative. The quantity  $P(\xi)$  should really be interpreted here as a kind of stress field of the vacuum. In the intuitive terms that would apply to a solid material object, this means that the vacuum can be either under internal compression (indicated by a positive pressure) or under internal traction (indicated by a negative pressure). If we consider the differential equations in Equations (36) through (38), using now the expression for the vacuum energy density in Schwarzschild coordinates given in Equation (50), that corresponds to a constant proper energy density of the vacuum, as well as the definition of the function  $\gamma(\xi)$  given in Equation (31), we have, in terms of dimensionless variables and function, that

$$\bar{\rho}(\xi) = \bar{\rho}_H \sqrt{\frac{\xi}{\xi - \gamma(\xi)}}, \quad (57)$$

where the dimensionless constant  $\bar{\rho}_H$  is given by

$$\bar{\rho}_H = \kappa r_0^2 \rho_H, \quad (58)$$

and using this expression for  $\bar{\rho}(\xi)$  we therefore get the set of three first-order differential equations

$$\gamma'(\xi) = \xi^2 \left[ \bar{\rho}_\Lambda + \bar{\rho}_H \sqrt{\frac{\xi}{\xi - \gamma(\xi)}} \right], \quad (59)$$

$$\bar{P}'(\xi) = - \frac{\gamma(\xi) + \xi^3 [\bar{P}(\xi) - \bar{\rho}_\Lambda]}{2\xi [\xi - \gamma(\xi)]} \left[ \bar{P}(\xi) + \bar{\rho}_H \sqrt{\frac{\xi}{\xi - \gamma(\xi)}} \right], \quad (60)$$

$$\nu'(\xi) = \frac{\gamma(\xi) + \xi^3 [\bar{P}(\xi) - \bar{\rho}_\Lambda]}{2\xi [\xi - \gamma(\xi)]}. \quad (61)$$

This is the set of equations that will be implemented numerically, still without a definite choice of value for  $\bar{\rho}_\Lambda$ . The effective total energy density of the vacuum shown in Equation (54), expressed in Schwarzschild coordinates, is now given by

$$\bar{\rho}_T(\xi) = \bar{\rho}_H \sqrt{\frac{\xi}{\xi - \gamma(\xi)}} + \bar{\rho}_\Lambda. \quad (62)$$

If we examine Equation (59), we see that this is the total energy density that appears there. In principle we could write these equations in the case of the choice for  $\bar{\rho}_\Lambda$  given by  $\bar{\rho}_\Lambda = -\bar{\rho}_H$ , which would work in infinite space. However, since in practice we cannot solve the equations numerically in an infinite interval of values of  $\xi$ , we will in fact deal with a slightly different set of equations, using a modified choice for  $\bar{\rho}_\Lambda$ , to be presented in Section 5, that will be solved within the finite interval  $(\xi_{M_1}, \xi_2]$ . This slightly different set of equations is what will generate the numerical results to be presented in this paper.

Besides the asymptotic boundary condition for  $\bar{\rho}(\xi)$  discussed above, leading to the necessity that we impose the condition that  $\bar{\rho}_\Lambda = -\bar{\rho}_H$  when working in infinite space, it is also necessary to discuss the corresponding condition for the vacuum stress function  $\bar{P}(\xi)$ . If we are to have that the whole subtracted stress-energy tensor  $\mathcal{T}_\mu^\nu$  of the vacuum becomes zero at radial infinity, so that we have an absolute vacuum there, then we can see from Equation (15) that we must also impose that  $\bar{P}(\xi) \rightarrow \bar{\rho}_\Lambda$  in that limit, that is, we must have that

$$\lim_{\xi \rightarrow \infty} \bar{P}(\xi) = \bar{\rho}_\Lambda, \quad (63)$$

so that in this limit the vacuum stress-energy tensor  $T_\mu^\nu$  acquires the same matrix structure as the cosmological term  $\rho_\Lambda g_\mu^\nu$ , being diagonal with all four diagonal components equal to  $\rho_\Lambda$ . Note however that we cannot impose this condition over all of spacetime, but only in the  $\xi \rightarrow \infty$  asymptotic limit. The function  $P(\xi)$  must be allowed to change, and will do so according to what the field equations determine. Note also that this implies that, at least for large values of  $\xi$ , the internal “pressure” within the vacuum is in fact negative, so that it is under “traction”, and not “compression”.

We must therefore solve the general-relativistic problem that we described above, including both the central mass  $M_1$  and the effective total energy density given by  $\rho_T(\xi)$ . Therefore, in general the solution in the vacuum region around and outside the distribution of normal matter will *not* be simply the exterior Schwarzschild solution, although it may *tend* to it asymptotically in the  $\xi \rightarrow \infty$  limit. In fact, in principle the solution may not even be flat space at radial infinity, but in the general case will tend instead to some curved cosmological solution, even with the inclusion of the cosmological term with a negative sign, if the cosmological constant  $\Lambda$  does not have exactly the required value.



## 5 Numerical Development of the Model

In order to enable the numerical approach to the problem it is of course essential that we reduce it to a finite interval of values of the radial variable  $\xi$ . Therefore, for the purposes of the detailed mathematical solutions obtained numerically and presented in this paper, we will assume that spacetime is completely empty, and hence in a state of absolute vacuum, with no normal matter and with no net proper vacuum energy density, beyond a certain outer radius  $\xi_2 = r_2/r_0$ , so that the solution becomes the exterior Schwarzschild solution for  $\xi \geq \xi_2$ , with an asymptotic gravitational mass parameter  $M_2$  that combines the mass  $M_1$  of the normal matter and the total equivalent mass given by the distribution of “dark matter” with the subtracted energy density  $\rho_{\mathcal{T}}(\xi)$  within the sphere centered at the origin with its surface passing by the radial position  $\xi_2$ . The outer radius  $r_2$  is to be interpreted as the radial position of the outer surface of the “dark-matter” halo. The exterior Schwarzschild solution is given, for all  $\xi \geq \xi_2$ , by the metric functions

$$\gamma(\xi) \equiv \xi_{M_2}, \quad (64)$$

$$e^{2\lambda(\xi)} = \frac{\xi}{\xi - \xi_{M_2}}, \quad (65)$$

$$e^{2\nu(\xi)} = \frac{\xi - \xi_{M_2}}{\xi}, \quad (66)$$

where  $\xi_{M_2} = r_{M_2}/r_0$  is the rescaled Schwarzschild radius  $r_{M_2} = 2GM_2/c^2$  of the mass  $M_2$ , as well as by the physical condition that the absolute-vacuum matter-energy functions be zero, as implied by the condition  $\mathcal{T}_\mu^\nu = 0$ , and hence by the conditions that  $\bar{\rho}_{\mathcal{T}}(\xi) = 0$  and that  $\bar{P}_{\mathcal{T}}(\xi) = 0$ , thus implying that

$$\bar{\rho}(\xi) \equiv -\bar{\rho}_\Lambda, \quad (67)$$

$$\bar{P}(\xi) \equiv \bar{\rho}_\Lambda, \quad (68)$$

also for all  $\xi \geq \xi_2$ . Therefore, we will impose at  $\xi_2$  certain boundary conditions that will have the effect of connecting the inner solution of the field equations shown in Equations (59) through (61), valid within the interval  $(\xi_{M_1}, \xi_2]$ , to the exterior Schwarzschild solution with asymptotic gravitational mass  $M_2$  for  $\xi \geq \xi_2$ .

In order to define a problem within this finite interval, that allows us not only to solve the equations but also to satisfy all the necessary boundary conditions, we have to adopt a slightly different choice for the constant  $\bar{\rho}_\Lambda$ , namely we will use the condition that

$$\begin{aligned} \bar{\rho}_\Lambda &= -\bar{\rho}_H e^{\lambda(\xi_2)} \\ &= -\bar{\rho}_H \sqrt{\frac{\xi_2}{\xi_2 - \xi_{M_2}}}. \end{aligned} \quad (69)$$

It is important to emphasize that this choice is *forced* upon us by the interface boundary conditions at  $\xi_2$ . For large  $\xi_2$ , such that  $\xi_2 \gg \xi_{M_2}$ , as is to be expected for low-density matter and energy distributions, this becomes very close to the condition  $\bar{\rho}_\Lambda = -\bar{\rho}_H$ . From Equation (62) we have now for the subtracted vacuum energy density

$$\bar{\rho}_{\mathcal{T}}(\xi) = \bar{\rho}_H \left[ \sqrt{\frac{\xi}{\xi - \gamma(\xi)}} - \sqrt{\frac{\xi_2}{\xi_2 - \xi_{M_2}}} \right]. \quad (70)$$

This leads to the final form of our set of three field equations, taken now to hold within the finite interval  $(\xi_{M_1}, \xi_2]$ , given by

$$\gamma'(\xi) = \xi^2 \bar{\rho}_H \left[ \sqrt{\frac{\xi}{\xi - \gamma(\xi)}} - \sqrt{\frac{\xi_2}{\xi_2 - \xi_{M_2}}} \right], \quad (71)$$

$$\bar{P}'(\xi) = - \frac{\gamma(\xi) + \xi^3 \left[ \bar{P}(\xi) + \bar{\rho}_H \sqrt{\frac{\xi_2}{\xi_2 - \xi_{M_2}}} \right]}{2\xi [\xi - \gamma(\xi)]} \left[ \bar{P}(\xi) + \bar{\rho}_H \sqrt{\frac{\xi}{\xi - \gamma(\xi)}} \right], \quad (72)$$

$$\nu'(\xi) = \frac{\gamma(\xi) + \xi^3 \left[ \bar{P}(\xi) + \bar{\rho}_H \sqrt{\frac{\xi_2}{\xi_2 - \xi_{M_2}}} \right]}{2\xi [\xi - \gamma(\xi)]}. \quad (73)$$

The numerical solutions to be presented in this paper are in fact exact solutions of these slightly modified equations, dully connected by the interface boundary conditions to the exterior Schwarzschild solution beyond  $\xi_2$ .

Let us now discuss in detail the boundary conditions to be imposed on  $\gamma(\xi)$ ,  $\bar{P}(\xi)$  and  $\nu(\xi)$  at  $\xi_2$ . The boundary condition for  $\gamma(\xi)$  is straightforward enough, we just integrate Equation (71) for  $\gamma(\xi)$  up to  $\xi_2$  and use the fact that, according to Equation (64), we have that  $\gamma(\xi_2) = \xi_{M_2}$  when  $\xi_2$  is approached from the right, a relation that we can use on the value of  $\gamma(\xi_2)$  obtained when approaching  $\xi_2$  from the left, in order to determine  $M_2$ , and then just use this value of  $M_2$  as the asymptotic gravitational mass parameter of the exterior Schwarzschild solution for  $\xi \geq \xi_2$ . This simple procedure guarantees the continuity of  $\gamma(\xi)$  across the exterior interface at  $\xi_2$ .

Having thus determined  $\gamma(\xi)$ , and hence  $\lambda(\xi)$ , within the interval  $(\xi_{M_1}, \xi_2]$ , we now use the fact that in the exterior Schwarzschild solution we have the well-known property that  $\nu(\xi) = -\lambda(\xi)$  in order to determine the value of  $\nu(\xi_2)$  when  $\xi_2$  is approached from the right. It is then a simple matter to add a constant to the function  $\nu(\xi)$  obtained numerically within the interval  $(\xi_{M_1}, \xi_2]$  so that we have that  $\nu(\xi) = \nu(\xi_2)$  at the outer interface, when  $\xi_2$  is approached from the left, thus guaranteeing the continuity of  $\nu(\xi)$ . This can be done in this simple way because the equation for  $\nu'(\xi)$  does not depend on  $\nu(\xi)$  itself, but only on  $\gamma(\xi)$  and  $\bar{P}(\xi)$ , as one can see in Equations (61) and (73), so that  $\nu(\xi)$  is given by just an integral involving only these other two functions, and hence we can always add to  $\nu(\xi)$  an integration constant without violating the equation determining  $\nu'(\xi)$  and therefore  $\nu(\xi)$ , that is, without violating Equations (61) and (73).

Note that these two boundary conditions can be trivially implemented if, instead of integrating forward either from a radial position close to  $\xi_{M_1}$  or from some position  $\xi_1$  above it, we integrate backward from a given value of  $\xi_2$ . This allows us to satisfy all the boundary conditions exactly, without having to rely on the relation between  $\xi_{M_1}$  and the mass function  $\gamma(\xi)$ , which is one reason why we will always use backward integration for the numerical results presented in this paper. For the integration leading to  $\gamma(\xi)$ , in this case we start at  $\xi_2$  with a given value of  $\xi_{M_2}$ , and hence with known values of the parameters  $\xi_2$ ,  $\xi_{M_2}$ ,  $\gamma(\xi_2) = \xi_{M_2}$  and  $\lambda(\xi_2)$  as given in Equation (31), and we just integrate  $\gamma(\xi)$  backward from that value at  $\xi_2$ . For the integration leading to  $\nu(\xi)$ , the known values of  $\xi_2$  and  $\xi_{M_2}$  lead at once to known values of  $\lambda(\xi_2)$  and  $\nu(\xi_2) = -\lambda(\xi_2)$ , and again we just integrate  $\nu(\xi)$  backward from that value at the exterior interface  $\xi_2$ .

Now to the more delicate question of the boundary condition for the vacuum stress function  $\bar{P}(\xi)$  at  $\xi_2$ . Given our choice for the parameter  $\bar{\rho}_\Lambda$ , shown in Equation (69), from Equations (67) and (68) it follows that the exterior Schwarzschild solution that we use for  $\xi \geq \xi_2$  corresponds to the conditions that  $\bar{\rho}(\xi)$  and  $\bar{P}(\xi)$  are constants, given by



$$\bar{\rho}(\xi) \equiv \bar{\rho}_H \sqrt{\frac{\xi_2}{\xi_2 - \xi_{M_2}}}, \quad (74)$$

$$\bar{P}(\xi) \equiv -\bar{\rho}_H \sqrt{\frac{\xi_2}{\xi_2 - \xi_{M_2}}}, \quad (75)$$

for all  $\xi \geq \xi_2$ , so that the total stress-energy tensor  $\mathcal{T}_\mu^\nu$  shown in Equation (15) is identically zero in that region, thus making it a region of absolute vacuum. However, according to Equation (57), we have for the energy density of the vacuum, when we approach the radial position  $\xi_2$  from the left, the value

$$\bar{\rho}(\xi_2) = \bar{\rho}_H \sqrt{\frac{\xi_2}{\xi_2 - \xi_{M_2}}}. \quad (76)$$

It follows therefore that the function  $\bar{\rho}(\xi)$  is continuous at  $\xi_2$ , since according to Equation (74) this is exactly the same value that we get when we come to  $\xi_2$  from the right. Note that, while a discontinuity of  $\bar{\rho}(\xi)$  may not disturb the differential system, since the derivative  $\bar{\rho}'(\xi)$  does not play a direct role in it, the derivative  $\bar{P}'(\xi)$  is in fact part of that system, so that a discontinuity of  $\bar{P}(\xi)$  would indeed disturb it. Something similar to the situation with regard to  $\gamma(\xi)$ , as described before, happens to the function  $\bar{P}(\xi)$ . Recalling that we have  $\bar{P}(\xi) \equiv -\bar{\rho}(\xi)$  for  $\xi \geq \xi_2$ , it follows from Equation (75) that we have

$$\bar{P}(\xi_2) = -\bar{\rho}_H \sqrt{\frac{\xi_2}{\xi_2 - \xi_{M_2}}}, \quad (77)$$

when we approach  $\xi_2$  from the absolute vacuum on the right. Therefore we can simply use this same value as the boundary condition when we integrate to the left from  $\xi_2$ , thus making the function  $\bar{P}(\xi)$  continuous at  $\xi_2$ . The only simple way to implement this condition is to use backward integration, starting from  $\xi_2$ , which is another reason why we will always use backward integration for the numerical results presented in this paper. In a similar way, we can now see that the continuity of  $\gamma(\xi)$ , and the continuity of  $\nu(\xi)$  as well, are simple consequences of the adoption of the boundary conditions at the exterior interface, that follow from Equations (64) and (66),

$$\gamma(\xi_2) = \xi_{M_2}, \quad (78)$$

$$e^{2\nu(\xi_2)} = \frac{\xi_2 - \xi_{M_2}}{\xi_2}. \quad (79)$$

Using the differential equations given in Equations (71) through (73), we can also verify that the derivatives of the three functions involved are also continuous at  $\xi_2$ . From Equation (71) we immediately get that  $\gamma'(\xi_2) = 0$  from the left, which is exactly the value of this quantity that we have from the right. From Equation (72), using the condition given in Equation (77), we immediately get that  $\bar{P}'(\xi_2) = 0$  from the left, which is exactly the value of this quantity that we have from the right. Finally, from Equation (73), again using the condition given in Equation (77), we get from the left that

$$\nu'(\xi_2) = \frac{\xi_{M_2}}{2\xi_2[\xi_2 - \xi_{M_2}]}, \quad (80)$$

which is exactly the result that we get from the right, from the exterior Schwarzschild solution, as can be easily verified by a straightforward calculation. Therefore the three

quantities involved in the field equations given in Equations (71) through (73), as well as their derivatives, are all continuous at  $\xi_2$ .

When integrating backward from  $\xi_2$ , there is the question of how to determine the value of  $\xi_{M_1}$ , leading to the mass  $M_1$  of the normal matter, which is the most crucial result that we still must determine, when integrating backward. In principle  $\xi_{M_1}$  could be obtained from the constant value of the function  $\gamma(\xi)$  near the left end of the interval  $(\xi_{M_1}, \xi_2]$ , but in this case this is somewhat uncertain. This is due to the fact that  $\rho\tau(\xi)$  is not exactly zero for  $\xi \approx \xi_{M_1\oplus}$ , which causes  $\gamma(\xi)$  not to be exactly constant in this region, thus making it more difficult to determine  $\xi_{M_1}$  from the behavior of this function. The fact that when we try to make  $\xi \rightarrow \xi_{M_1\oplus}$  we are in fact approaching a coordinate singularity of this system of coordinates also complicates things somewhat.

Fortunately, there is a fairly simple and sensitive alternative method for doing this. Once we calculate the orbital velocity  $v_\phi(\xi)$ , we will see that it displays a clear and rather dramatic change of behavior when we pass from one side to the other of the  $(\xi_{M_1}, \xi_2]$  interval. There are two separate regions of values of  $\xi$ , in each one of which the behavior of  $v_\phi(\xi)$  is quite different. The behavior of  $v_\phi(\xi)$  morphs continuously from one behavior to the other along the interval, but both are very well characterized, one at each end. While on the right-hand side of the interval the velocity  $v_\phi(\xi)$  tends to be either constant or to vary quite slowly with  $\xi$ , on the left-hand side of it  $v_\phi(\xi)$  tends to decrease relatively quickly with  $\xi$ , as one would expect to be the case for the exterior gravitational field of a tightly localized central mass  $M_1$ , as given in Equation (48).

Note that this change of strategy consists of giving up using  $\gamma(\xi)$  in favor of using  $v_\phi(\xi)$  for the purpose of the determination of  $\xi_{M_1}$ . Note also that using  $\gamma(\xi)$ , which is related to  $\lambda(\xi)$ , in order to determine  $\xi_{M_1}$ , corresponds to using the spatial part of the geometry for this purpose, while using  $v_\phi(\xi)$ , which is related to  $\nu(\xi)$ , corresponds to using the temporal part of the geometry for the same purpose. As it happens, in this case using the temporal part is conceptually clearer, easier and more precise. Once  $\xi_{M_1}$  is determined in this way, we can compare the resulting value to that obtained from the function  $\gamma(\xi)$ , at least approximately, given that we have that  $\gamma(\xi) \rightarrow \xi_{M_1}$  when  $\xi \rightarrow \xi_{M_1\oplus}$ . We will see that these two evaluations of  $\xi_{M_1}$  turn out to be in fact quite close to one another.

In order to describe the method for the measurement of  $\xi_{M_1}$  from  $v_\phi(\xi)$ , let us recall that close to the left end of the interval  $(\xi_{M_1}, \xi_2]$  we have the gravitational field of some central distribution of normal matter with total mass  $M_1$ , which has the property that  $v_\phi(\xi)$  falls off at least approximately as  $1/\sqrt{\xi}$  outside that distribution, just like it does in the case of the exterior Schwarzschild solution beyond the radial position  $\xi_2$ , as shown in Equation (48). We therefore can obtain the value of  $\xi_{M_1}$ , and hence the value of  $M_1$ , from the behavior of  $v_\phi(\xi)$  in that region. As it turns out, we can obtain  $\xi_{M_1}$  quite precisely by means of a process of linear regression applied to the leftmost part of the graph of  $[v_\phi(\xi)/c]$ , which in this region can be approximated with very good precision by the expression

$$\left[ \frac{v_\phi(\xi)}{c} \right]^2 = \alpha + \xi_{M_1} \left( \frac{1}{2\xi} \right), \quad (81)$$

which is a linear expression in terms of the variable  $\chi = 1/(2\xi)$ . The second term in the sum on the right-hand side of this expression is the expectation for the behavior of the squared orbital velocity in the case of a central mass  $M_1$ , and the first term is a correction due to the fact that the subtracted universal vacuum energy density still exists in the whole  $(\xi_{M_1}, \xi_2]$  interval, and even within the smaller central region where the mass  $M_1$  of the normal matter is distributed.

A very interesting additional relation can be obtained from the fact that the exterior

Schwarzschild solution holds for  $\xi \geq \xi_2$ , and from the necessity that  $v_\phi(\xi)$  be continuous at  $\xi_2$ . Given the mass  $M_2$ , the exterior Schwarzschild solution for  $\xi \geq \xi_2$  is known, and therefore so is the form of  $v_\phi(\xi)$  in this region, namely we have the relation given in Equation (48). If  $v_{\phi,0}$  is the approximately constant value of  $v_\phi(\xi)$  in a neighborhood to the left of  $\xi_2$ , then the continuity of this function at  $\xi_2$  results in the relation

$$\frac{v_{\phi,0}}{c} = \sqrt{\frac{\xi_{M_2}}{2\xi_2}}. \quad (82)$$

There is, therefore, a fixed relation between  $v_{\phi,0}$ ,  $\xi_{M_2}$  and  $\xi_2$ . Given  $v_{\phi,0}$  and  $\xi_{M_2}$ , two quantities that are easily accessible and well known in many cases, the position  $\xi_2$  of the exterior interface is determined. This allows us to use as input data only the three parameters  $\bar{\rho}_H$ ,  $v_{\phi,0}$  and  $\xi_{M_2}$ , the last two of which are the most directly and immediately observable, and then derive from them all the rest of the structure of the solution.

At this point it is important to point out that the choice of value for  $\bar{\rho}_\Lambda$  made in Equation (69) means that the specific problem to be solved numerically here is no more than an approximation of the physics conceptually involved in the model as described in Section 4. This is so because, if we assume that  $\bar{\rho}_H$  is an universal physical constant, then it follow from Equation (69) that  $\bar{\rho}_\Lambda$  is not, and vice versa, since that relation involves the radius  $\xi_2$  of the halo and the Schwarzschild radius  $\xi_{M_2}$  of the galaxy and halo, which are not universal constants. Note that the choice of the value of  $\bar{\rho}(\xi)$  for  $\xi > \xi_2$  adopted in Equation (69) is slightly *larger* than the asymptotic choice  $\bar{\rho}(\infty) = \bar{\rho}_H$  introduced in Section 4.

However, although strictly speaking this discrepancy is present, one can show that the distortion introduced by Equation (69) on the values of the universal constants  $\bar{\rho}_\Lambda$  and  $\bar{\rho}_H$  is very small. Let us first show that this distortion can be written in terms of the fractional orbital velocity ( $v_{\phi,0}/c$ ) given in Equation (82). If we consider the difference of the quantities involved in these two choices of  $\bar{\rho}_\Lambda$ , and write it as a variation of  $\bar{\rho}_H$ , we have from Equation (69) that

$$\begin{aligned} \Delta\bar{\rho}_H &= \bar{\rho}_H \sqrt{\frac{\xi_2}{\xi_2 - \xi_{M_2}}} - \bar{\rho}_H \\ &= \bar{\rho}_H \left[ \sqrt{\frac{1}{1 - (\xi_{M_2}/\xi_2)}} - 1 \right]. \end{aligned} \quad (83)$$

Since we certainly have that  $\xi_{M_2}/\xi_2 \ll 1$ , we can expand this expression in terms of this variable, around zero, thus obtaining

$$\frac{\Delta\bar{\rho}_H}{\bar{\rho}_H} = \frac{\xi_{M_2}}{2\xi_2}. \quad (84)$$

However, according to Equation (82), the right-hand side of this relation is the square of the fractional orbital velocity, so that we have

$$\frac{\Delta\bar{\rho}_H}{\bar{\rho}_H} = \left( \frac{v_{\phi,0}}{c} \right)^2. \quad (85)$$

The values of  $v_{\phi,0}$  seem to be typically below 300 km/s, in which case we always have that

$$\frac{\Delta\bar{\rho}_H}{\bar{\rho}_H} < 10^{-6}, \quad (86)$$

so that the distortion is indeed quite small, and hence does not prevent the approximate numerical model from being potentially useful.

For greater flexibility in the use of the program, we chose to write the main program to solve the equations in the form given in Equations (59) through (61), without a fixed choice for the relation between the parameters  $\rho_\Lambda$  and  $\rho_H$ . A second program was written to prepare the input for this first program, giving the user alternatives for the choice of the parameters and of the boundary conditions, so as to implement the solutions of the set of field equations given in Equations (71) through (73), and possibly of some variations of them. This operates as a small front-end program to the main program. We can organize these equations as a set of equations that are only partially coupled to one another, as seen in Equations (59) through (61) and in Equations (71) through (73), which are written in coupling order. For the numerical integration procedure in the main program we define the two auxiliary functions given by

$$F_1(\xi, \gamma) = \sqrt{\frac{\xi}{\xi - \gamma(\xi)}}, \quad (87)$$

$$F_2(\xi, \gamma, \bar{P}) = \frac{\gamma(\xi) + \xi^3 [\bar{P}(\xi) - \bar{\rho}_\Lambda]}{2\xi [\xi - \gamma(\xi)]}, \quad (88)$$

the first of which is just another name for the metric coefficient function  $\exp[\lambda(\xi)]$ , and then the numerical development equations can be written in a fairly simple way as

$$\delta\gamma(\xi) = \left\{ \xi^2 [\bar{\rho}_\Lambda + \bar{\rho}_H F_1(\xi, \gamma)] \right\} \delta\xi, \quad (89)$$

$$\delta\bar{P}(\xi) = \left\{ -F_2(\xi, \gamma, \bar{P}) [\bar{P}(\xi) + \bar{\rho}_H F_1(\xi, \gamma)] \right\} \delta\xi, \quad (90)$$

$$\delta\nu(\xi) = \left\{ F_2(\xi, \gamma, \bar{P}) \right\} \delta\xi. \quad (91)$$

This set of three finite-difference equations can be solved by means of the Runge-Kutta fourth-order algorithm in a straightforward way. We did this in a couple of illustrative cases, meant to put in evidence the main properties of the solutions, thus obtaining the results that we present in the Section 6.

## 6 Numerical Results

In this section we will present a few numerical results obtained for one particular set of input parameters for the problem. This set was designed to result in a solution with the main general properties found in galaxy halos. Namely, we tried to reproduce a value of approximately 0.15 for the  $(\xi_{M_1}/\xi_{M_2}) = (M_1/M_2)$  ratio, and an orbital velocity curve with the approximately constant value  $v_{\phi,0} \approx 220$  km/s in the central interval of values of  $r$ . This is targeted at establishing the qualitative compatibility of the model with typical galactic data. The values of the dimensionless parameters used for this purpose were  $\bar{\rho}_H = 1.4 \cdot 10^{-2}$ ,  $\xi_{M_2} = 1.1 \cdot 10^{-4}$  and  $\xi_2 = 100$ , the last of which just corresponds to the choice of a value for the arbitrary radial parameter  $r_0$ , namely the value  $r_0 = r_2/100$ .

From this choice of input parameters we can already obtain an estimate for the value of the energy density of the vacuum. From Equation (58), multiplying through by  $\xi_{M_2}^2$ , we have for the vacuum energy density

$$\begin{aligned}
\rho_H &= \frac{\bar{\rho}_H \xi_{M_2}^2}{\kappa r_{M_2}^2} \\
&= \frac{\bar{\rho}_H \xi_{M_2}^2 c^8}{32\pi G^3 M_2^2},
\end{aligned} \tag{92}$$

where we have substituted the values of  $\kappa = 8\pi G/c^4$  and  $r_{M_2} = 2GM_2/c^2$ . Using the values of  $\bar{\rho}_H$  and  $\xi_{M_2}$  given above, and using  $M_2 = 2.4457 \cdot 10^{42}$  kg, which is the approximate total mass of the Andromeda galaxy, including the equivalent mass of the “dark matter” halo, this results in approximately  $\rho_H = 61.8$  J/m<sup>3</sup>, which quite surprisingly is compatible with the human scale. This value is approximately 11 orders of magnitude above the currently accepted estimate of the cosmological value of approximately  $5.3566 \cdot 10^{-10}$  J/m<sup>3</sup>, but we must recall that the cosmological value is related, not simply to  $\rho_H$ , but to the possibly very small difference between the two commensurate quantities  $\rho(\xi)$  and  $|\rho_\Lambda|$ .

It is also possible to calculate the radius of the halo for the set of values of parameters that we use here. We have that  $r_2 = r_0 \xi_2$  can be written in terms of  $r_{M_2} = r_0 \xi_{M_2}$  as

$$\begin{aligned}
r_2 &= \frac{\xi_2}{\xi_{M_2}} r_{M_2} \\
&= \frac{\xi_2}{\xi_{M_2}} \frac{2GM_2}{c^2},
\end{aligned} \tag{93}$$

where we have substituted the value of  $r_{M_2} = 2GM_2/c^2$ . Using the values of  $\xi_2$  and  $\xi_{M_2}$  given above, and once more the value  $M_2 = 2.4457 \cdot 10^{42}$  kg, which is the approximate total mass of the normal matter and the “dark matter” halo of the Andromeda galaxy, this expression results in approximately  $r_2 = 349049$  light-years. This is just about 4.6 times the radius of the disk of the Andromeda galaxy.

The main numerical program implements the Runge-Kutta fourth-order algorithm to solve the three differential equations shown in Equations (59) through (61). It runs in quadruple precision mode, that is, using 128-bits real numbers, in any machine with a 64-bit architecture. The integration interval used was  $\delta\xi = 10^{-6}$ , and the run took approximately 33 min on a run-of-the-mill 2.6 GHz personal desktop computer. The program used here is freely available online on the Internet, and can be found at the Internet site shown in [8], from which it can be easily downloaded.

Let us start by commenting about some aspects of the solution that are not directly reported in the graphs shown here. Remarkably, up to the numerical precision used in the numerical resolution of the equations, the value of the vacuum stress function  $\bar{P}(\xi)$  remains essentially constant throughout the integration, at the negative value  $\bar{P}(\xi_2) = \bar{\rho}_\Lambda$  used for the interface boundary condition at  $\xi_2$ , from that position right down to the region close to  $\xi_{M_1}$ . Since the value of  $\bar{\rho}_\Lambda$  is also a constant, this implies that the subtracted pressure  $P_{\mathcal{T}}(\xi)$ , which from Equation (55) is the difference of these two, is in fact very nearly zero throughout the solution. If we consider  $P_{\mathcal{T}}(\xi)$  to be the total stress function of the vacuum, that takes into account the pressures from both the energy density of the vacuum and the cosmological constant, then this implies that in this solution the vacuum is neither under compression nor under traction, but rather in a non-stressed state.

In stark contrast to this, the subtracted vacuum energy density  $\bar{\rho}_{\mathcal{T}}(\xi)$  is not at all constant, but decreases quickly with  $\xi$ . Near the Schwarzschild radius  $\xi_{M_1}$  it falls off approximately as  $1/\xi$ , and further to the right it tends to fall off progressively faster than that, approaching  $1/\xi^2$  as we get close to  $\xi_2$ . Note that the behavior  $1/\xi^2$  is the one that results from a classical Newtonian analysis, for all values of  $\xi$ . Since this is not the case in the solution presented here, we see that, although a galaxy corresponds to a very low-density

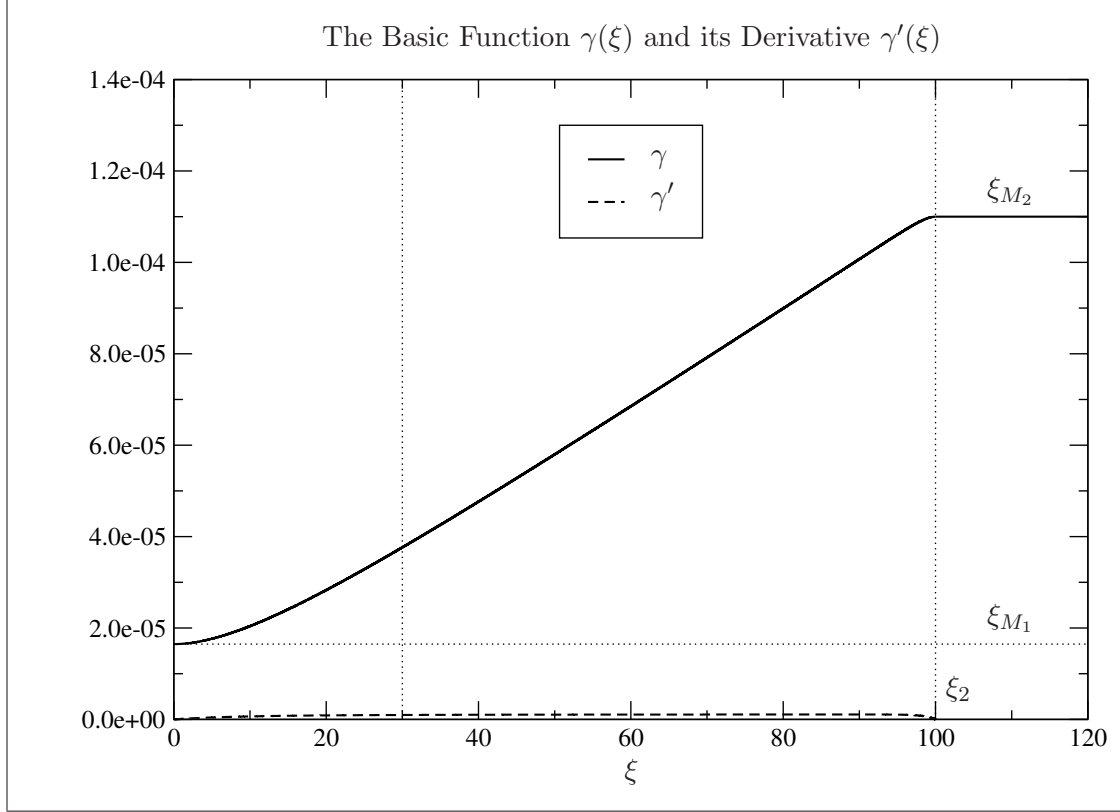


Figure 1: Graph of the basic function  $\gamma(\xi)$  and its derivative  $\gamma'(\xi)$ . The light vertical dotted line on the left marks the separation of the region where the effect of the central mass  $M_1$  dominates, to its left, and the region where the effect of the halo dominates, to its right. The other light vertical dotted line marks the position of  $\xi_2$ . To the right of  $\xi_2$  we see the exterior Schwarzschild solution for the total mass  $M_2$ . The light horizontal dotted line marks the value of  $\xi_{M_1}$ , and on the extreme left the solution tends to this constant.

average distribution of matter, it is still essential that we use General Relativity for the analysis, despite the commonly held belief that Newtonian gravitation is always sufficient for low-density systems. In Figures from 1 through 4 we present the results from this run, for the main functions involved in the solutions.

In Figure 1 one can see the graph of the function  $\gamma(\xi)$  resulting from the numerical resolution, as well as of its derivative  $\gamma'(\xi)$ . The position of the outer interface  $\xi_2$  is marked by a light vertical dotted line, and the value of the Schwarzschild radius  $\xi_{M_1}$  is marked by a light horizontal dotted line. The position at  $\xi = 30$  is also marked by a light vertical dotted line, and defines the approximate boundary between two regions regarding the behavior of  $[v_\phi(\xi)/c]$ , the region to its left, where the effect of the central mass  $M_1$  dominates the dynamics, which we will name the *inner region*, and the region to its right, where the effect of the halo dominates, which we will name the *intermediate region*.

As one can see in the graph, in the outer region, for  $\xi \geq \xi_2$ , we have the constant value of  $\gamma(\xi)$  for the exterior Schwarzschild solution, at the value  $\xi_{M_2}$  that corresponds to the total mass  $M_2$ . In the intermediate region we have that  $\gamma(\xi)$  increases very approximately linearly with  $\xi$ . This represents the main part of the halo region. Note that as  $\xi \rightarrow \xi_{2\ominus}$  the function  $\gamma(\xi)$  connects to the exterior Schwarzschild solution with zero derivative, so that both the function and its derivative are continuous. In the inner region we have the

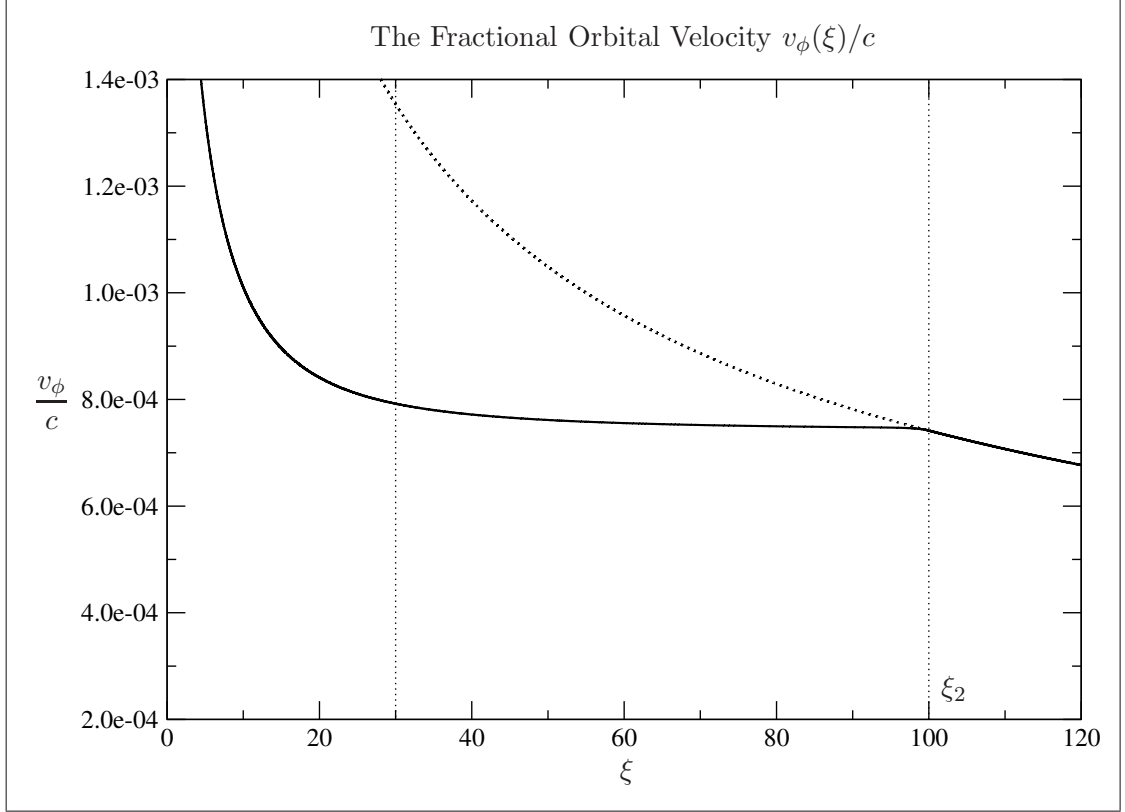


Figure 2: Graph of the fractional orbital velocity curve, given by the function  $[v_\phi(\xi)/c]$ . The light vertical dotted line on the left marks the separation of the region where the effect of the central mass  $M_1$  dominates, to its left, and the region where the effect of the halo dominates, to its right. The other light vertical dotted line marks the position of  $\xi_2$ . To the right of  $\xi_2$  we see the behavior of the exterior Schwarzschild solution due to the total mass  $M_2$ , that for illustrative purposes is shown extended to the left. On the extreme left the behavior is that of another Schwarzschild-like solution, this one due to the mass  $M_1$  of the normal matter.

behavior of  $\gamma(\xi)$  that corresponds essentially to the gravitational field of a central mass  $M_1$ . As we make  $\xi \rightarrow \xi_{M_1 \oplus}$  the function  $\gamma(\xi)$  approaches the value  $\xi_{M_1}$  with either zero or very small derivative. This corresponds to the exterior Schwarzschild solution for the central mass  $M_1$ , but it is not necessarily exact because the halo still exists in this region.

As one can see, the numerical program propagates without difficulty almost down to the position given by the Schwarzschild radius  $\xi_{M_1}$ , that is, close to the position of the possible event horizon associated with the central mass  $M_1$  of the normal matter. In a more realistic setting the central matter distribution with total mass  $M_1$  will be in fact a wide and low-density distribution, instead of a dense central mass, and then the radius of that distribution is not related in any way to the value of  $\xi_{M_1}$  obtained here in the way described in Section 5 and shown in Figure 3.

In Figure 2 one can see the graph of the function  $[v_\phi(\xi)/c]$  resulting from the numerical resolution. The position of  $\xi_2$  and the approximate position  $\xi = 30$  of the boundary between the inner and intermediary regions are marked by light vertical dotted lines. Once again one can see that the program propagates flawlessly and smoothly, from  $\xi_2$  right down to a position very close to  $\xi_{M_1}$ , the position of the possible event horizon associated with the central mass  $M_1$  of the normal matter.



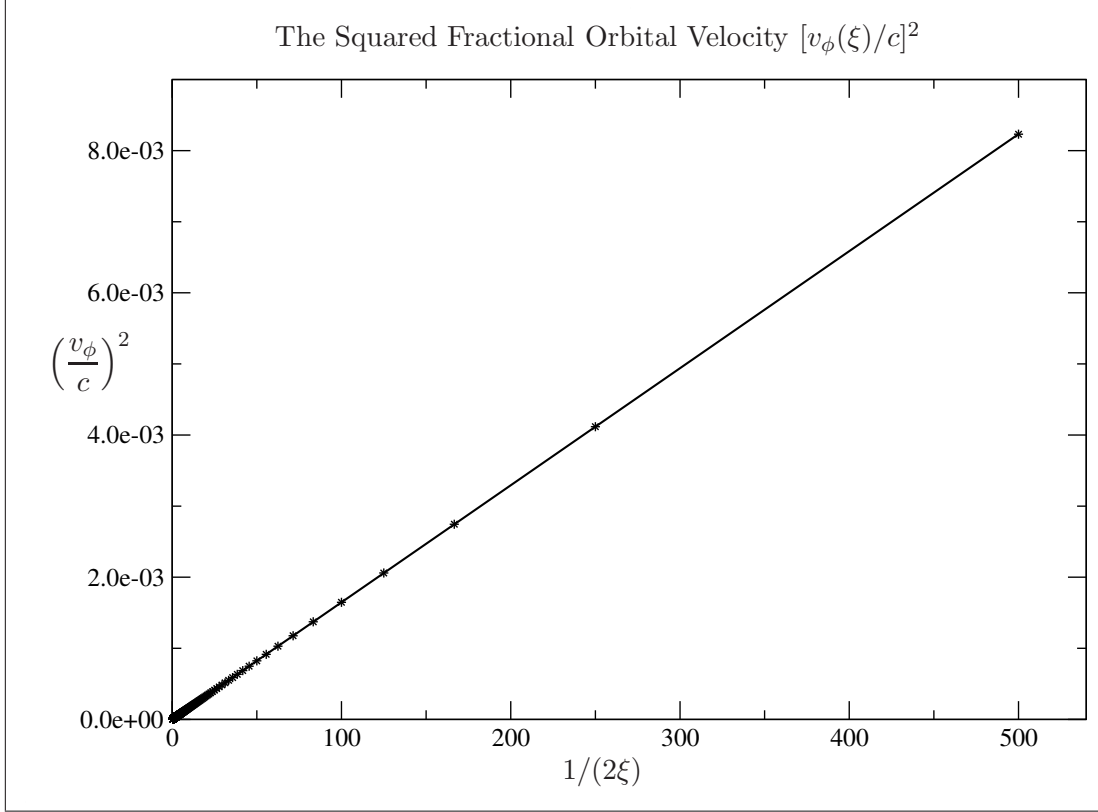


Figure 3: Graph of the squared fractional orbital velocity  $(v_\phi/c)^2$  as a function of  $1/(2\xi)$ , with the data points marked by small stars. The result of the linear regression to the right end of this graph, applied to the last 33 of the  $10^5$  points of this graph, from which the value of  $\xi_{M_1}$  is obtained, is also shown, using a solid line. The value obtained from the fit, for the value  $\xi_{M_1}$  of the Schwarzschild radius associated with the mass of the normal matter, is  $\xi_{M_1} = 1.6463 \cdot 10^{-5}$ . The left end of the regression gets very close to the origin.

As one can see in the graph, in the outer region, for  $\xi \geq \xi_2$ , we have the behavior of  $[v_\phi(\xi)/c]$  given in Equation (48) for the exterior Schwarzschild solution, with the value  $\xi_{M_2}$  that corresponds to the total mass  $M_2$ . In this case this function was extended to the left, as seen in the heavy dotted curve, for illustrative purposes. In the intermediate region, for  $\xi \in [30, 100]$ , we have that  $[v_\phi(\xi)/c]$  is approximately constant at the average value  $7.5904 \cdot 10^{-4}$ , a little above the value  $7.4162 \cdot 10^{-4}$  that it assumes exactly at  $\xi_2$ , as a consequence of the values chosen for the parameters  $\xi_2$  and  $\xi_{M_2}$ . This represents the main halo region, and this average value corresponds to an average orbital velocity of approximately 228 km/s. It is visually clear that  $[v_\phi(\xi)/c]$  is continuous and differentiable, with a continuous derivative, at the interface  $\xi_2$ . In the inner region, for  $\xi < 30$ , we have the behavior of  $[v_\phi(\xi)/c]$  given in Equation (81), which for the smaller values of  $\xi$  approximates the behavior of the exterior Schwarzschild solution, for the value  $\xi_{M_1}$  that corresponds to the total mass  $M_1$  of the normal matter. Therefore, as we make  $\xi \rightarrow \xi_{M_1}$  we approach the relativistic gravitational field of a central mass  $M_1$ .

In Figure 3 one can see a graph of the quantity  $(v_\phi/c)^2$  plotted as a function of  $1/(2\xi)$ , which was used in order to execute the linear regression of the expression shown in Equation (81). The process of linear regression was applied to the last 33 points of the  $10^5$  points in the graph shown, from the value 15 to the value 500 of the quantity  $1/(2\xi)$ . The



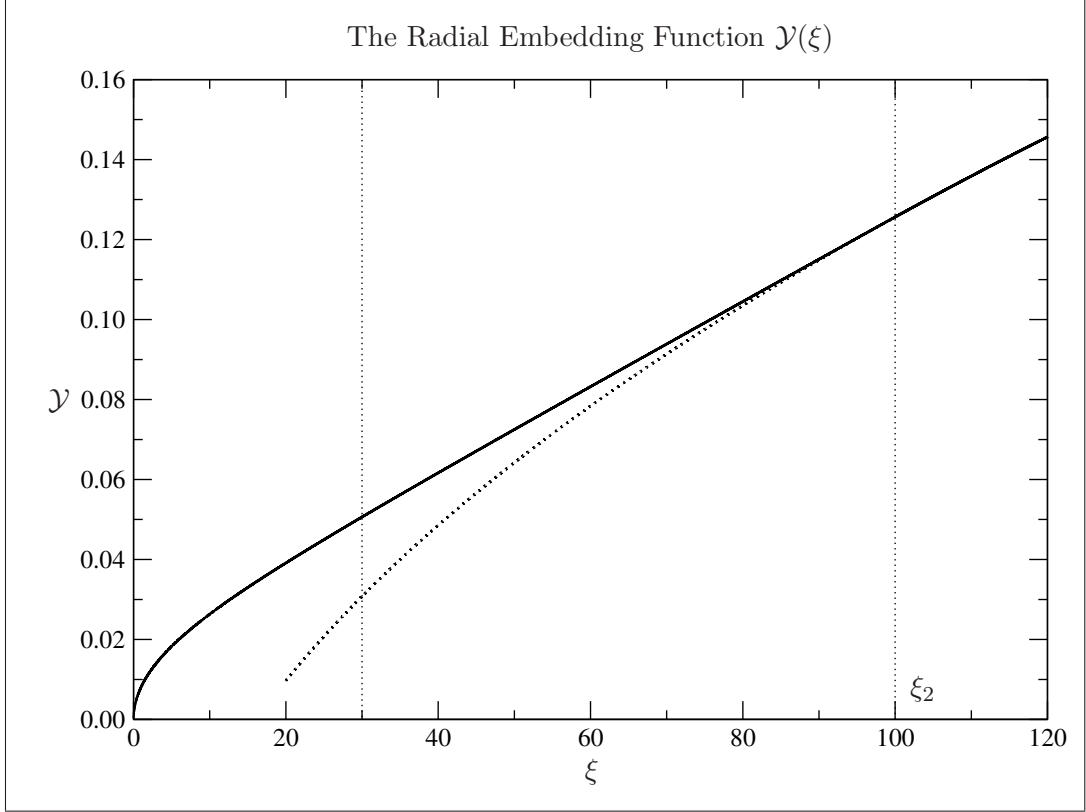


Figure 4: The radial embedding of a section through the origin of the spatial geometry. The light vertical dotted line on the left marks the separation of the region where the effect of the central mass  $M_1$  dominates, to its left, and the region where the effect of the halo dominates, to its right. The other light vertical dotted line marks the position of  $\xi_2$ . To the right of  $\xi_2$  we see the behavior due to the total mass  $M_2$ , a piece of a paraboloid of revolution that for illustrative purposes is shown extended to the left. On the extreme left we see another paraboloid, this one associated with the mass  $M_1$  of the normal matter.

result of the regression is shown as a solid line, and the data points are marked with small stars. The linear fit is essentially perfect within the numerical precision used, which is the double precision level (that is, using 64-bit real numbers), with a correlation coefficient of 1. From the fit we get the values  $\xi_{M_1} = 1.6463 \cdot 10^{-5}$  for the slope and  $\alpha = 5 \cdot 10^{-7}$  for the intercept. The corresponding value obtained from the  $\xi \rightarrow \xi_{M_1}$  limit of the function  $\gamma(\xi)$  is approximately  $\xi_{M_1} = 1.6478 \cdot 10^{-5}$  for  $\xi = 10^{-3}$ , so that the difference is given by  $1.5 \cdot 10^{-8}$  and the relative error is of the order of  $9 \cdot 10^{-4}$ , or slightly less than 0.1%. The corresponding value of the ratio  $(\xi_{M_1}/\xi_{M_2})$  turns out to be  $(\xi_{M_1}/\xi_{M_2}) = 0.1497$ .

We present also an embedding of the spatial geometry in a fictitious three-dimensional Euclidean space, as shown in Figure 4, which is an useful way to represent in an intuitive way the character of the spatial part of the solution. This is done for a two-dimensional spatial section through the origin, for  $\theta = \pi/2$ , which is described therefore by the Schwarzschild coordinates  $r$  and  $\phi$ . The embedding function  $\mathcal{Y}(\xi)$  is defined by assuming that there is a variable  $\mathcal{Y}$  that satisfies the condition that  $d\ell^2 = d\xi^2 + d\mathcal{Y}^2$ , where  $d\ell^2 = \exp[2\lambda(\xi)]d\xi^2$  is the square of the rescaled proper length. This implies that we have

$$d\mathcal{Y}^2 = \left[ e^{2\lambda(\xi)} - 1 \right] d\xi^2, \quad (94)$$

and therefore, if we integrate from some point  $\xi_0$ , that we have in terms of  $\gamma(\xi)$

$$\mathcal{V}(\xi) = \int_{\xi_0}^{\xi} d\xi' \sqrt{\frac{\gamma(\xi')}{\xi' - \gamma(\xi')}}. \quad (95)$$

The result is shown in Figure 4, with a choice of  $\xi_0$  such that the vertex of the horizontal-axis parabola in the inner region is very close to the  $\mathcal{V} = 0$  axis. The embedding as shown here is possible because we have that  $0 < \gamma(\xi) < \xi$ , which implies that  $\lambda(\xi) > 0$  and hence that  $\exp[2\lambda(\xi)] > 1$ . This is the same condition that guarantees that  $\bar{\rho}_T(\xi) > 0$ .

As one can see in the graph, in the outer region we find the well-known arc of parabola with an horizontal axis, which is the usual embedding of the geometry given by the exterior Schwarzschild metric, representing the gravitational field of the total mass  $M_2$  in an absolute vacuum. In this case the arc of the horizontal-axis parabola was extended to the left, as seen in the heavy dotted curve, for illustrative purposes. In the intermediate region, between  $\xi = 30$  and  $\xi = 100$ , the function  $\mathcal{V}(\xi)$  turns out to be approximately linear, indicating that this section corresponds to an approximately conical embedding. This region contains most of the energy of the halo. In the inner region we have once again an arc of parabola with an horizontal axis, but this time only approximately so, since the halo does extend to this region, so that we do not have an absolute vacuum there. This corresponds very closely to the geometry of the gravitational field of a localized central mass, in this case the total mass  $M_1$  of the normal matter. The horizontal arc of parabola approaches the  $\mathcal{V} = 0$  axis at the point  $\xi = \xi_{M_1}$ , which is too close to zero to be visually identifiable in the graph.

The numerical program, which is freely available online as shown in [8], can be used to produce many more such examples, with parameters that can be tailored to any required physical situation. This can be done in any average personal computer, in a small amount of time. As it is presently written, the program requires as inputs the values of  $\bar{\rho}_H$ ,  $\xi_{M_2}$  and  $\xi_2$ . The default values correspond to the results reported in the graphs shown in Figures 1 through 4. Alternatively, with the use of Equation (82), we can redefine the input data to be given in terms of  $\bar{\rho}_H$ ,  $\xi_{M_2}$  and  $(v_{\phi,0}/c)$ , the last two of which can be taken as the two most basic properties of any “dark-matter” halo, namely its total mass and its constant orbital velocity. The program then produces, of course, all the relevant functions of the solution for the given set of input parameters. The main resulting observables in this second approach are the Schwarzschild radius  $\xi_{M_1}$  and the outer radial position  $\xi_2$ , from which one can get the ratio  $(\xi_{M_1}/\xi_{M_2})$  and the overall size of the halo. It is interesting to observe that the numerical evidence indicates that, so long as we keep both  $\bar{\rho}_H$  and  $\xi_2$  constant, changes in  $\xi_{M_2}$  do not change this ratio at all, since  $\xi_{M_1}$  turns out to be proportional to  $\xi_{M_2}$ , so as to keep the ratio constant. The only dimensionless parameter that changes when one changes  $\xi_{M_2}$  in this way is the value of the orbital velocity  $(v_{\phi,0}/c)$ .

## 6.1 A Small Experiment

In the graph shown in Figure 5 we indulge ourselves in a small mathematical experiment. This graph corresponds to a second run of the numerical program in which we implement a small deformation of the boundary condition for the vacuum stress function  $\bar{P}(\xi)$  at the  $\xi_2$  interface. In this case we use for the interface boundary condition, which in any case can be written as  $\bar{P}(\xi_2) = \bar{\rho}_\Lambda$ , instead of the choice of  $\bar{\rho}_\Lambda$  given in Equation (69), a linear combination of that choice with the choice  $\bar{\rho}_\Lambda = -\bar{\rho}_H$  which is valid in infinite space, thus resulting in the deformed interface boundary condition given by

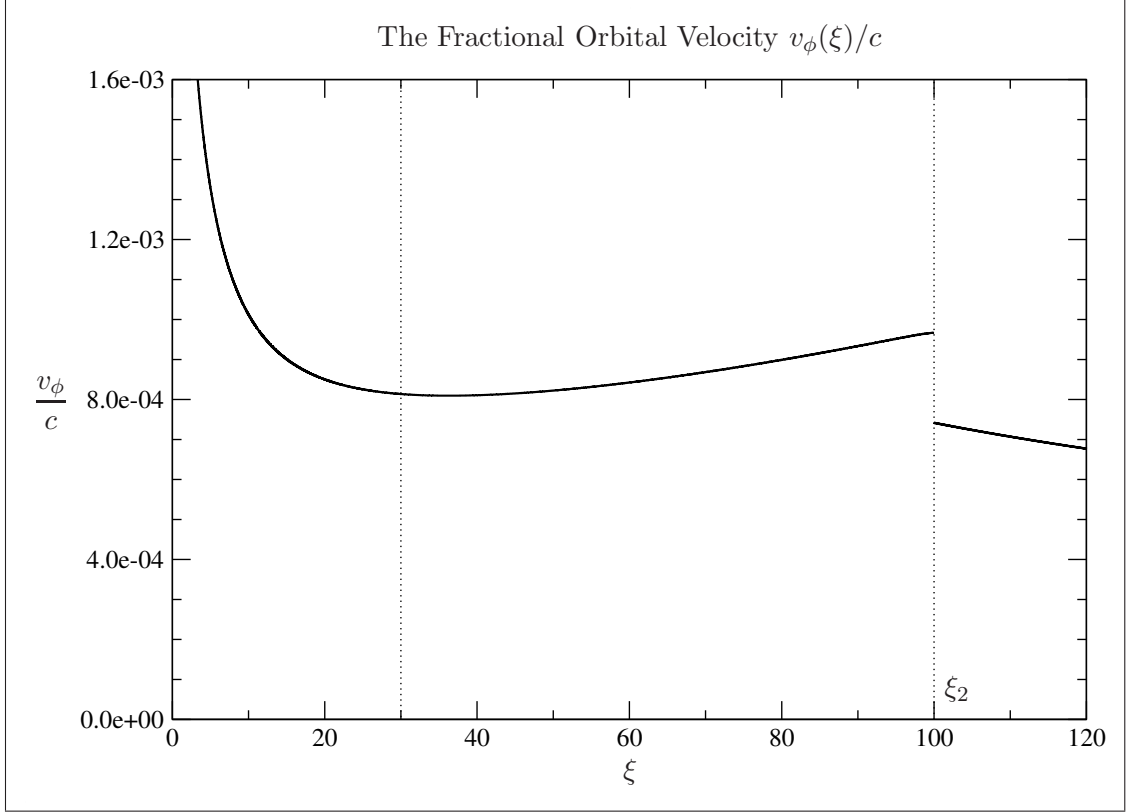


Figure 5: Graph of the fractional orbital velocity curve, given by the function  $[v_\phi(\xi)/c]$ , with slightly distorted boundary conditions for  $\bar{P}(\xi_2)$ . The level of distortion used was  $\varepsilon = 0.01$ . The light vertical dotted line on the left marks the separation of the region where the effect of the central mass  $M_1$  dominates, to its left, and the region where the effect of the halo dominates, to its right. The other light vertical dotted line marks the position of  $\xi_2$ . To the right of  $\xi_2$  we see the exterior Schwarzschild solution for the total mass  $M_2$ . On the extreme left the behavior is that of another Schwarzschild-like solution, this one due to the mass  $M_1$  of the normal matter.

$$\bar{P}(\xi_2) = -\bar{\rho}_H \left[ (1 - \varepsilon) \sqrt{\frac{\xi_2}{\xi_2 - \xi_{M_2}}} + \varepsilon \right]. \quad (96)$$

The values of the remaining parameters and interface boundary conditions are the same as before. This reduces to the previous case for  $\varepsilon = 0$ , and reproduces the choice in infinite space for  $\varepsilon = 1$  and  $\xi_2 \rightarrow \infty$ . The run shown in the graph presented in Figure 5 was done with  $\varepsilon = 10^{-2}$ , which corresponds to a 1% level of deformation.

Note that this change in the interface boundary condition on  $\bar{P}(\xi)$  at  $\xi_2$  has no effect at all on the solutions for  $\gamma(\xi)$  and  $\lambda(\xi)$ , so that the results shown in the graphs of Figures 1 and 4 do not change, and hence apply to this case as well. As it turns out, it has also no significant effect on the behavior of  $[v_\phi(\xi)/c]$  at the left end of the interval  $(\xi_{M_1}, \xi_2]$ , leading to exactly the same evaluation of  $\xi_{M_1}$  obtained in the previous case, within the numerical precision used. In fact, the whole linear regression process returns exactly the same results, within the numerical precision used, so that both the slope and the intercept turn out to be the same, and therefore Figure 3 applies to this case as well.

One can also check that the interface boundary conditions for all relevant functions,

$\gamma(\xi)$ ,  $\bar{P}(\xi)$  and  $\nu(\xi)$  are still valid, and even that the derivatives of  $\gamma(\xi)$  and  $\bar{P}(\xi)$  are still continuous. The single condition that is violated by the deformation is that on the derivative  $\nu'(\xi)$  of  $\nu(\xi)$ . Although the condition of the continuity of the derivative  $\nu'(\xi)$  may not be directly implied or required by the differential equations in their current form, as they are shown in Equations (59) through (61), it is nonetheless an important condition on physical grounds. Besides, unlike what happens in the case of the second derivative  $\lambda''(\xi)$ , the second derivative  $\nu''(\xi)$  does show up during the algebraic manipulations leading from the general form of the equations as shown in Equation (11) to the particular form of the equations shown in Equations (59) through (61), so that it is essential that  $\nu'(\xi)$  be differentiable and therefore continuous.

As one can see in the graph of Figure 5, in the outer region we have the same solution as before, namely the exterior Schwarzschild solution with the mass  $M_2$ , which has not changed. In the intermediate region, however, we see a clear difference, since the value of  $[v_\phi(\xi)/c]$  tends now to increase somewhat from left to right along that region. In the inner region there is no significant change, that is, we have an approximate Schwarzschild solution, with an approximation that improves as we go towards the left end of the region. We can still use the fit to the expression shown in Equation (81), thus obtaining exactly the same results for  $\xi_{M_1}$  and  $\alpha$ .

The other notable difference introduced by this second run is the discontinuity of  $[v_\phi(\xi)/c]$  at  $\xi_2$ , which is due to a corresponding discontinuity of  $\nu'(\xi)$ , and which is clearly not acceptable from the point of view of the physics. The discontinuity depends in a quite sensitive way on the deformation. With a relative deformation of the boundary condition given by  $\varepsilon = 0.01$ , we have for  $[v_\phi(\xi)/c]$  at either side of the discontinuity the values  $9.6695 \cdot 10^{-4}$  and  $7.4162 \cdot 10^{-4}$ , leading to a difference of  $2.2533 \cdot 10^{-4}$  and hence to a relative difference of 0.3038. In other words, with a 1% deformation of the boundary conditions, we get a much larger 30% relative discontinuity of the function  $[v_\phi(\xi)/c]$  at  $\xi_2$ .

Despite this difficulty, this experiment does show that the differential system has the capacity to generate a slightly increasing value of  $[v_\phi(\xi)/c]$  in the halo region, as is sometimes observed. This can be obtained with a fairly small deformation, in this case we have a 1% deformation leading to an approximately 30% relative discontinuity of  $[v_\phi(\xi)/c]$ , and to a correspondingly significant positive variation of  $[v_\phi(\xi)/c]$  along the interval. In order to realize this scheme in a physically more realistic way, it is probably necessary to exchange the exterior Schwarzschild solution in the outer region for some other solution, in order to have all the necessary continuity conditions satisfied.

## 7 Conclusions

In this paper we have shown that the qualitative characteristics of galactic “dark-matter” halos, as established by the astronomical observations, can be correctly accounted for by a fairly simple model that relies only on a few well-established facts from quantum field theory and the structure of the Einstein theory of general relativity. The single fundamental hypothesis involved is the existence of an universal proper energy density of the vacuum, which is due to the spontaneous symmetry breaking mechanism of the quantum field theory that underlies the standard model of elementary particle physics. The introduction of the so-called cosmological term in the Einstein field equations, which is done here for reasons other than the usual cosmological ones, also has a fundamental role to play, since it corresponds either to a change in the usual form of that theory, or to the introduction of a new type of source of gravity, namely a scalar source. It is noteworthy that, since both the proper energy density and the cosmological constant are intrinsically constant, in different ways,

the distribution of the net energy density is determined by the Einstein field equations, and does not depend on any particular form of material particle dynamics, as it would if the halo was made of material particles.

In building the model it is important to keep in mind that there is a clear physical distinction between the cosmological constant  $\Lambda$  and the proper energy density  $\rho_H$  of the vacuum, despite the fact that the cosmological constant can be redefined as  $\rho_\Lambda$  so that it acquires the same physical dimensions that  $\rho_H$  has. The physical effects pointed out in this paper come from the interplay of these two quantities, that have different transformation properties under coordinate transformations, since one is a scalar and the other is the  $T_0^0$  component of a rank-2 tensor. The energy density of the vacuum belongs squarely in the source side of the Einstein field equations, and therefore involves no changes in the standard theory. However, the cosmological term can be interpreted either as a term in the field side of the equations, or as a term in the source side. Therefore, the issue of whether this model corresponds to a change in the original Einstein theory, or to just the inclusion of a different type of source, remains an open one. Either interpretation is possible.

All the other hypotheses made during the development of the model have a merely circumstantial character, and are meant only as simplifications of the problem, so as to allow us to actually find the solutions. The resulting simplified model can be adjusted to reproduce correctly the two main characteristics of any galactic halo, namely the ratio  $(M_1/M_2)$ , of the total mass of only the normal matter, by the total mass including the equivalent mass of the halo, and the approximately constant value  $(v_{\phi,0}/c)$  of the orbital velocity as a function of the radial position within the halo, which characterizes the so-called velocity curve. Of course the numerical results presented here cannot be considered as a complete representation of any real galactic data, since most of the structure of a typical galaxy has been ignored in this mathematical exercise, such as the stellar disk and the gaseous halo. In Subsection 7.1 below we will point out some ways in which this model could possibly be improved.

Of the three input parameters necessary for the model, two represent directly the main observable characteristics of the galactic halos. One is the total mass  $M_2$  of the galaxy, including both the mass  $M_1$  of the normal matter and the equivalent mass of the subtracted vacuum energy distribution  $\rho_T(\xi)$  of the halo. The other can be chosen to be either the outer radius  $r_2$  of the halo, or the value  $(v_{\phi,0}/c)$  of the constant orbital velocity. The third input parameter is the value of the constant proper energy density  $\rho_H$ . Using some typical galactic data for an approximate estimate, namely data for the Andromeda galaxy, this turns out to be approximately  $62 \text{ J/m}^3$ , a number that turns out to be quite commensurate with the human scale, but that is some 11 orders of magnitude above the currently accepted estimate of the cosmological value. This is not surprising, because in this model the cosmological value is not given simply by the vacuum energy density, but by the difference  $\rho_H - |\rho_\Lambda|$ , which can be arbitrarily small. In fact, in the results presented here the model has been adjusted to result in zero for this difference, in the  $r \rightarrow \infty$  asymptotic limit. If there is some special significance to the number obtained for  $\rho_H$ , it is currently unknown to us.

One result that follows from the model and that can be easily verified against the observations is that expressed in Equation (82), which gives a fixed relation among three observable quantities, the Schwarzschild radius  $r_{M_2}$  of the total mass of the galaxy and halo, the external radius  $r_2$  of the halo, and the constant orbital velocity  $(v_{\phi,0}/c)$ . It is our understanding that, while  $r_{M_2}$  and  $(v_{\phi,0}/c)$  are relatively well-known, the same cannot be said of  $r_2$ . In this case the relation in Equation (82) may provide hints about where to look for the outer edge of the halo. Another quantity that can be estimated by means of the model, using the same typical galactic data, is the outer radius  $r_2$  of the halo, as shown in

Equation (93), and which in the example used for the calculation, that of the Andromeda galaxy, turns out to be about 4.6 times the radius of the disk of the galaxy. This is another result that it should be eventually possible to verify against the observations.

One important aspect of the model is that it involves and contrasts two different concepts of vacuum, one being the particle vacuum of quantum field theory and the other being the absolute vacuum of general relativity. The model promotes the idea that we can have a particle vacuum that is not an absolute vacuum, due to the presence of the universal energy density following from the vacuum expectation value of the Higgs field. Since this is a form of energy that is not connected to the presence of particles, it therefore tends to shift the emphasis of the interpretation from particles to fields, in the quantum field theory of elementary particles. One advantageous property of this model is that, since it formulates the explanation of the halos in terms of a continuous distribution of energy, rather than by postulating the existence of new particles of matter, it completely eliminates the need to search for such new particles. Since this search has been going on for many years with no positive results at all, we have good reason to believe that the fundamental hypotheses leading to this model are somewhat closer to the truth.

## 7.1 Outlook

There are, of course, several ways in which the model presented here could be improved. For one thing, one could try to improve the representation of the structure of the galaxy, taking into consideration its multiple elements, such as the disk and the gaseous and stellar halos. The detailed consideration of the disk would probably be the most difficult, since it violates spherical symmetry in favor of an axial symmetry, and would therefore require a complete reworking of the mathematics from the basic principles. However, a least two improvements of the model suggest themselves as more amenable to the type of mathematical treatment given in this paper. One of them would involve the left end of the intermediate halo region, which is in contact with the inner region. This would consist of the detailed consideration of the central bulge, with the exchange of the single central body of normal matter by some form of extended solution for the distribution of normal matter, and the implementation of interface boundary condition on an inner interface at a radial position  $r_1$ .

In this case it is clear that the divergent behavior of  $[v_\phi(r)/c]$  when  $r \rightarrow r_{M_1}$  in the inner region would be changed to a limit to zero as  $r \rightarrow 0$ , as one would expect for an extended low-density distribution of normal matter. In this case the value of  $r_{M_1}$  would no longer be measured, but would instead be encoded into the solution to be adopted in the inner region. The result would probably become a lot closer to the usual behavior observed for  $[v_\phi(r)/c]$ , namely a rise from zero at  $r = 0$  to a constant value throughout the intermediate region of the halo. Since the theory is deeply non-linear, the change caused by this improvement may not be limited to the inner region, but might affect the results within the intermediate halo region as well.

For the other type of improvement that is possible, let us consider now the other end of the intermediate halo region, that which is in contact with the outer region. As we discussed in Subsection 6.1 the deformation of the interface boundary condition for  $P(r)$  at  $r_2$  produces a value of  $[v_\phi(r)/c]$  in the intermediate halo region that increases somewhat with  $r$ , but also results in a discontinuity of  $[v_\phi(r)/c]$  at  $r_2$ , if we try to use the exterior Schwarzschild solution in the outer region. This discontinuity of  $[v_\phi(r)/c]$  is due to a corresponding discontinuity of the derivative  $\nu'(r)$  at that point. Therefore, it is not possible to connect the deformed solution within the halo region, in a completely continuous and differentiable way, to the exterior Schwarzschild solution in the outer region. The discon-



tinuity of the derivative  $\nu'(r)$  is the only condition that is violated by the deformation of the interface boundary condition, but this is enough to render that solution physically untenable.

It would seem that the only possible solution to this problem is the replacement of the exterior Schwarzschild solution in the outer region. However, since the exterior Schwarzschild solution is the unique static and spherically symmetric vacuum solution that corresponds to a flat spacetime at radial infinity, it follows that in order to produce a solution with an increasing value of  $[v_\phi(r)/c]$  within the halo region we must use in the outer region a solution leading to some small amount of curvature left over in the  $r \rightarrow \infty$  asymptotic limit. For example, one could consider using a static and spherically symmetric solution that could represent approximately, in a sufficiently large local region around the galaxy, and for a short amount of time when compared to the age of the universe, a curved cosmological solution. In this case there will be no exact cancellation of the terms involving  $\bar{\rho}_H$  and  $\bar{\rho}_\Lambda$  in the outer region, leading to a small constant value of the difference of their absolute values, and thus leading in turn to a small constant value of the subtracted energy density  $\bar{\rho}_T(r)$  left over in the outer region. If this program can be carried out, it will result in a connection of our local galactic problem involving the “dark matter” halos with the cosmological problem involving the concept of “dark energy”.

We end by noting that in the specific realization of the model presented here the position of the outer radius  $r_2$  of the halo is being abstracted from the observational data for  $(v_{\phi,0}/c)$  and  $r_{M_2}$ , and that we do not have an *ab initio* derivation of it. If there is indeed such a sharp interface, representing a sudden transition in the state of the vacuum, it is probably due to the quantum properties of the vacuum itself. Any exploration into that would most likely be a very difficult one, and would probably involve a rather difficult and complex calculation in quantum field theory.

## Data Availability Statement

Data sharing not applicable to this article as no datasets were generated or analyzed during the current study.

## Conflict of Interest Statement

The authors hereby certify that there are no actual or potential conflicts of interest of any of the authors in relation to this article.

## References

- [1] C. Quigg, *Gauge Theories of the Strong, Weak and Electromagnetic Interactions*. Princeton University Press, second ed., September 22 2013. 504 pages, ISBN: 9781400848225, <https://doi.org/10.1515/9781400848225>, <https://www.jstor.org/stable/j.ctt3fgx94>.
- [2] F. Halzen and A. D. Martin, *Quarks and Leptons: an Introductory Course in Modern Particle Physics*. Wiley, first ed., January 16 1991. 396 pages, ISBN-10: 0471887412, ISBN-13: 978-0471887416.
- [3] P. A. M. Dirac, *General Theory of Relativity*. John Wiley & Sons, Inc., 1975. ISBN 0-471-21575-9.

- [4] R. Wald, *General Relativity*. University of Chicago Press, 2010.
- [5] C. W. Misner, K. S. Thorne, and J. A. Wheeler, *Gravitation*. San Francisco: W.H. Freeman and Co., 1973.
- [6] J. L. deLyra, R. de A. Orselli, and C. E. I. Carneiro, “Exact solution of the einstein field equations for a spherical shell of fluid matter,” *General Relativity and Gravitation*, vol. 55, no. 5, 2023. Article ID: 68; DOI: 10.1007/s10714-023-03116-5.
- [7] J. L. deLyra, “Complete solution of the einstein field equations for a spherical shell of truly incompressible liquid,” *General Relativity and Gravitation*, 2024. DOI: 10.1007/s10714-024-03262-4.
- [8] J. L. deLyra, “Program for a three-parameter model for dark matter halos based on general relativity and quantum field theory.” DOI/Zenodo.

## A Table of Connection Components

The values of the components of the Christoffel connection  $\Gamma^\mu_{\nu\sigma}$  for a static and spherically symmetric geometry, in Schwarzschild coordinates.

$$\begin{aligned}
 \Gamma^0_{\nu\sigma} &= \begin{bmatrix} 0 & \nu'(r) & 0 & 0 \\ \nu'(r) & 0 & 0 & 0 \\ 0 & 0 & 0 & 0 \\ 0 & 0 & 0 & 0 \end{bmatrix}, \\
 \Gamma^1_{\nu\sigma} &= \begin{bmatrix} \nu'(r) e^{2\nu(r)-2\lambda(r)} & 0 & 0 & 0 \\ 0 & \lambda'(r) & 0 & 0 \\ 0 & 0 & -r e^{-2\lambda(r)} & 0 \\ 0 & 0 & 0 & -r \sin^2(\theta) e^{-2\lambda(r)} \end{bmatrix}, \\
 \Gamma^2_{\nu\sigma} &= \begin{bmatrix} 0 & 0 & 0 & 0 \\ 0 & 0 & r^{-1} & 0 \\ 0 & r^{-1} & 0 & 0 \\ 0 & 0 & 0 & -\sin(\theta) \cos(\theta) \end{bmatrix}, \\
 \Gamma^3_{\nu\sigma} &= \begin{bmatrix} 0 & 0 & 0 & 0 \\ 0 & 0 & 0 & r^{-1} \\ 0 & 0 & 0 & \cot(\theta) \\ 0 & r^{-1} & \cot(\theta) & 0 \end{bmatrix}.
 \end{aligned}$$